AFOSR Interim Scientific Report

AD 750014

A THEORETICAL STUDY OF SPHERICAL GASEOUS DETONATION WAVES

by

W.H. Kyong
G.G. Bach
J.H. Lee
R. Knystautas

MERL Report 72-7

Research sponsored by Air Force Office of Scientific Research
Office of Aerospace Research,
United States Air Force

Col. R.W. Haffner, AFOSR Technical Monitor

AFOSR Grant 69-1752B

Department of Mechanical Engineering
McGill University
Montreal, Canada

Reproduced by
NATIONAL TECHNICAL
INFORMATION SERVICE
U S Department of Commerce
Springfield VA 22151

July 1972

UNCLASSIFIED

Security Classification

DOCUMENT CONTROL DATA - R & D

(Security classification of title, body of abstract and indexing annotation must be entered when the overall report is classified)

1. ORIGINATING ACTIVITY (Corporate author)
MCGILL UNIVERSITY
DEPARTMENT OF MECHANICAL ENGINEERING
MONTREAL 110, P.Q., CANADA

2a. REPORT SECURITY CLASSIFICATION
UNCLASSIFIED

2b. GROUP

3. REPORT TITLE

A THEORETICAL STUDY OF SPHERICAL GASEOUS DETONATION WAVES

4. DESCRIPTIVE NOTES (Type of report and inclusive dates)
Scientific Interim

5. AUTHOR(S) (First name, middle initial, last name)

WON H KYONG JOHN H LEE GLEN G BACH ROMAS KNYSTAUTAS

6. REPORT DATE
July 1972

7a. TOTAL NO. OF PAGES
47

7b. NO. OF REFS
34

8a. CONTRACT OR GRANT NO.
AFOSR-69-1752

b. PROJECT NO.
9711-01

c. 61102F

d. 681308

9a. ORIGINATOR'S REPORT NUMBER(S)
MERL Report 72-7

9b. OTHER REPORT NO(S) (Any other numbers that may be assigned this report)
AFOSR - TR - 72 - 1927

10. DISTRIBUTION STATEMENT

Approved for public release; distribution unlimited.

11. SUPPLEMENTARY NOTES

TECH, OTHER

12. SPONSORING MILITARY ACTIVITY
AF Office of Scientific Research (NAE)
1400 Wilson Boulevard
Arlington, Virginia 22209

13. ABSTRACT

Numerical solutions using the Hartree characteristic method for the propagation of spherical blast waves in a detonation gas are presented in the present paper. Two models have been studied, the reacting blast wave (R-B-W) model and the finite kinetic rate (F-K-R) model. For the R-B-W model, the present numerical solution is used as a reference to assess the accuracies and the domains of validity of the various existing analytical solutions (i.e., quasi-similar method of Oshima, perturbation method of Melnikova and Sakurai and the density profile method of Porzel). The present solution also confirms the result of Levin and Chernyi in that the C-J state is reached at a finite radius for cylindrical and spherical waves. The asymptotic formula of Levin and Chernyi also predicts the correct value for the C-J radius. However, it is found from the present solution that the J-T-Z similarity solution as assumed by Levin and Chernyi is not recovered in the limit as the C-J state is reached. A new asymptotic decay law is proposed and found to be independent of the flow gradients to the first order in $\varepsilon^{\frac{1}{2}}$ and is identical to Levin and Chernyi's formula. The finite kinetic solution reveals all the essential qualitative features of a spherical combustion wave. Quantitative predictions of the shock and reaction front trajectories as well as the critical energy for direct initiation are correlated with previous experimental data. Based on a blast wave model for a multiheaded detonation front, the present F-K-R solution is used to predict the transverse wave spacings.

DD FORM 1 NOV 65 1473

UNCLASSIFIED

14. KEY WORDS	LINK A ROLE	LINK A WT	LINK B ROLE	LINK B WT	LINK C ROLE	LINK C WT
THEORETICAL NUMERICAL SOLUTION						
SPHERICAL GASEOUS DETONATIONS						
REACTING BLAST WAVE MODEL						
FINITE KINETIC RATE MODEL						

AFOSR - TR - 72 - 1927

AFOSR Scientific Report

A THEORETICAL STUDY OF SPHERICAL GASEOUS DETONATION WAVES

by

W.H. Kyong

G.G. Bach

J.H. Lee

R. Knystautas

DDC
RECEIVED
OCT 20 1972
B

MERL Report 72-7

Progress report for research sponsored in part by the United States Air Force Office of Scientific Research, Col. R.W. Haffner, Technical Monitor under AFOSR Grant 69-1752B and by the National Research Council of Canada under Grants A-3347, A-118 and A-7091.

Approved for public release;
distribution unlimited.

Department of Mechanical Engineering
McGill University
Montreal, Canada

ic

July 1972

ABSTRACT

Numerical solutions using the Hartree characteristic method for the propagation of spherical blast waves in a detonation gas are presented in the present paper. Two models have been studied, the reacting blast wave (R-B-W) model and the finite kinetic rate (F-K-R) model. The R-B-W model assumes the reaction rates to be infinitely fast, and the reactive shock wave is treated as a discontinuity. In the F-K-R model the double front approximation is used. Empirical relationships for the dependence of the induction time on reactant concentrations and thermodynamic states used in the present calculation are taken from the experimental work of White and Strehlow. The location of the reaction front is determined using the quasi-steady kinetic approximation as proposed by Strehlow. For the R-B-W model, the present numerical solution is used as a reference to assess the accuracies and the domains of validity of the various existing analytical solutions (i.e., quasi-similar method of Oshima, perturbation method of Melnikova and Sakurai and the density profile method of Porzel). It is found that the density profile method of Porzel is the most accurate as well as having the widest range of validity for both the parameters at the shock and the flow profiles behind the blast. The present solution also confirms the result of Levin and Chernyi in that the C-J state is reached at a finite radius for cylindrical and

spherical waves. The asymptotic formula of Levin and Chernyi also predicts the correct value for the C-J radius. However, it is found from the present solution that the J-T-Z similarity solution as assumed by Levin and Chernyi is not recovered in the limit as the C-J state is reached. Instead the solution tends towards the planar solution. A new asymptotic decay law is proposed and found to be independent of the flow gradients to the first order in $\varepsilon^{\frac{1}{2}}$ and is identical to Levin and Chernyi's formula. Hence it clarifies the correctness of Levin and Chernyi's asymptotic law which is based on an incorrect assumption of the asymptotic form of the solution since the C-J radius is independent of the flow gradient. The finite kinetic solution reveals all the essential qualitative features of a spherical combustion wave. Quantitative predictions of the shock and reaction front trajectories as well as the critical energy for direct initiation are correlated with previous experimental data. Based on a blast wave model for a multiheaded detonation front, the present F-K-R solution is used to predict the transverse wave spacings.

1. Introduction

The propagation of blast waves in a detonating gas has received considerable attention in the past decade [1-13]. The majority of the theoretical studies are of the analytical type where the classical point blast similarity solution of Taylor [14] and Sedov [15] is extended to account for the energy release due to chemical reactions. In these reacting blast wave (R-B-W) models, the detonation front is assumed to be a discontinuity (i.e., infinite reaction rates), hence all the non-similar techniques [16-18] developed for non-reacting blast waves with counter-pressure effects are directly applicable to the R-B-W model [1, 3, 7, 9, 11]. All these non-similar solutions of the R-B-W model account for small departures from the strong point blast similarity solution and hence break down as the initially overdriven blast wave approaches the Chapman-Jouguet (C-J) condition. Their validity is restricted to the regime where the shock radius R_s is small as compared to the characteristic explosion length R_0 (i.e., $R_s/R_0 < 1$). It is one of the aims of the present paper to assess the extent of validity of the non-similar analytical solutions in terms of the numerical solution of the R-B-W model presented herein. The asymptotic motion as the blast approaches the C-J state has been analysed by Levin and Chernyi [5] with the rather surprising conclusion that while a planar reacting blast decays to a C-J wave asymptotically (i.e., $M_s \to M_{CJ}$ as $R_s \to \infty$) a cylindrical or spherical reacting blast wave approaches the C-J state at a

finite radius (i.e., $M_s \rightarrow M_{CJ}$ as $R_s \rightarrow R_{CJ}$). Levin and Chernyi's asymptotic decay law is based on the assumption that as the blast wave approaches the C-J state the solution tends to the classical Jouguet [19]-Taylor [20]-Zeldovich [21] (J-T-Z) similarity solution for a diverging C-J detonation. It is not at all obvious that the flow gradients behind a decaying blast should steepen and become infinite at the C-J state as described by the J-T-Z similarity solution. Hence in the present paper it seemed worthwhile to verify this asymptotic decay law of Levin and Chernyi by comparing it with an exact numerical solution of the R-B-W model. It is particularly interesting to see if the flow gradients behind the decaying blast do indeed steepen and take on the J-T-Z profiles as the C-J state is reached.

In an effort to understand the chemical reactions in the transient hydrodynamic flow structure of a decaying blast wave, theoretical studies on a finite kinetic rate (F-K-R) model have been made [6, 22, 23]. These studies are of an analytical nature where the hydrodynamics and the chemical kinetics are decoupled by assuming that the heat released by chemical reactions has a negligible influence on the motion of the blast wave. Based on this assumption, the hydrodynamic flow structure can be obtained from the non-similarity solution of a non-reacting blast, and with the flow structure known the kinetic rate equations can then be integrated to establish the reaction profiles and induction time behind the blast wave. Such analytical solutions exclude a priori the all-important

coupling mechanisms between the energy released by chemical reactions and the hydrodynamic flow field. Hence these solutions cannot throw light on the interesting experimental observations such as the re-establishment phenomenon and the existence of a critical energy for direct initiation. The present paper also describes the result of a numerical solution of the F-K-R model. The theoretical predictions of the various propagation regimes of a reacting blast, the dependency of the critical energy for direct initiation on the initial condition of the explosive system as well as the dimensions of transverse wave spacings of multiheaded detonation waves using the blast wave model are compared with existing experimental results.

2. Theoretical Models and Method of Solution

The basic model is that of a point spherical blast wave propagating in a detonating gas. In the reacting blast wave (R-B-W) formulation, the reaction rates are assumed to be infinitely fast so that in effect the chemical reactions release the energy, Q per unit mass, right at the shock front which is treated as a discontinuity. In the finite kinetic rate (F-K-R) formulation, the two-front approximation used by Bishimov, Korobeinikov and Levin [10], is adopted. The two-front model assumes that the chemical energy Q is released at the reaction front only. The reaction front trails behind the leading shock front by an induction distance. The location of the reaction front is determined by the standard quasi-steady kinetic method

first used by Strehlow [24] in his study of the propagation of a reaction shock wave in a converging channel and later used by Bach, Knystautas and Lee [22], Lundstrom and Oppenheim [6], and Bishimov, Korobeinikov and Levin [10] in their studies of the F-K-R model. The empirical experimental relationship for the dependence of the induction time on the fuel-oxygen concentrations and the thermodynamic variables, i.e.,

$$\log(\tau_i [O_2]^m [fuel]^{l-m}) = A + \frac{B}{RT} \tag{2.1}$$

are used. In the numerical solution of the gasdynamic equations, the Hartree characteristic method as used by Chou and Huang [25] in their numerical solution for a non-reacting blast wave is adopted in the present work. The perfect gas constant γ assumption is used throughout the present study. The details of the basic conservation equations, the Rankine-Hugoniot relationships for the reacting shock front as well as the method of computation using the Hartree characteristic scheme have already appeared in journal publications. It suffices here to mention the appropriate references [3, 25].

3. Comparison with Analytical Solutions for the R-B-W Model

Existing analytical solutions for the R-B-W model are based on the following non-similar techniques developed to account for counter-pressure effects in non-reacting blast

waves: i) the quasi-similar technique of Oshima, ii) the perturbation solution of Melnikova and Sakurai and iii) the power-law density profile method of Porzel. Oshima's method was first used by Lee [1] for the R-B-W model in 1965 and later by Struck [9] and Brossard [11]. The method is based on the assumption that the flow field is locally similar. Hence the partial differential gasdynamic equations are reduced to ordinary differential equations based on the instantaneous shock strength. Oshima's method conserves the total energy, hence shock trajectories and the variation of shock strength with radius are adequately described. However, the flow structure behind the blast wave is poorly predicted since the method fails to conserve the total mass enclosed by the blast at any instant. The method of Melnikova and Sakurai is based on perturbing the similarity solution of Taylor and Sedov for the strong point blast. The solution is written in the form of a power series in $1/M_s^2$. This perturbation method was used by Korobeinikov [7] and Bach and Lee [3] for the R-B-W model. The method is rigorous but due to the asymptotic nature of the perturbation expansion, the solution diverges rapidly as the blast decays to the C-J condition. The power-law density profile method was originally suggested by Porzel [18] and developed by Rae [26] and Bach and Lee [27]. The method assumes the form of the density profile behind the blast wave to be given by a simple power-law form. Then from the conservation of mass and momentum equations, the forms for the particle velocity and the pressure profiles

can be obtained. The complete solution is obtained using the known profiles in the energy integral. This method was applied to the R-B-W model by Bach and Lee [3] and found to be an extremely accurate method even as the blast approaches the C-J condition. In comparing the present solution with these various analytical solutions, the particular case of stoichiometric C_2H_2-O_2 mixture at an initial pressure of 100 torr and at room temperature is used. Thus Fig. 1 compares the variation of shock strength $\eta' = (M_{CJ}/M_s)^2$ with shock radius R_s/R_0 from the various analytical solutions with the present numerical solution. It can be seen that for the relatively strong reacting blast regime (i.e., $0 \leq \eta' < .25$) all the analytical solutions are almost identical to the numerical solution. Departures from the exact numerical solution occur in the range $.25 \leq \eta' \leq 1$. The density profile method of Porzel yields a solution that follows closely to the numerical solution throughout the entire range $0 \leq \eta' \leq 1$.

In Fig. 2, the pressure profiles behind the reacting blast wave for various blast radii from the analytical solutions are compared with the present numerical solution. For the relatively strong blast regime (i.e., $0 \leq \eta' \leq .4$) the profiles from the perturbation and the Porzel solutions are almost identical to the exact numerical solution. For the region close to the shock front, the profiles using Oshima's method are identical to those from the numerical solution; however, they begin to deviate progressively from

it as one approaches the center of symmetry. For the regime of moderate shock strength, the perturbation solution retains the close agreement with the exact solution. Porzel's method yields a good description of the profile near the front but predicts a lower value for the pressure near the center of symmetry. All the analytical solutions break down in the asymptotic regime as $M_s \rightarrow M_{CJ}$ except the method of Porzel which still yields an adequate approximate description.

The density distribution behind the decaying reactive blast is shown in Fig. 3. Except for the very strong blast regime where $\eta' \leq .25$, the perturbation solution fails to provide an adequate description of the density distribution. For $\eta' \geq .5$, the second order perturbation solution over-corrects the first order solution and the density ratio at the front itself deviates significantly from the correct value. The asymptotic nature of the perturbation series is thereby demonstrated in this figure. Again the method of Porzel yields a fairly good description down to the asymptotic regime as $M_s \rightarrow M_{CJ}$.

The particle velocity profiles are shown in Fig. 4. We can see that as a consequence of failing to conserve mass, the particle velocity profile deviates significantly from the present numerical solution in the moderate blast strength regime (i.e., $\eta' \simeq .8$). Porzel's method once again is quite adequate in the asymptotic regime as $M_s \rightarrow M_{CJ}$.

In general from the η' vs R_s/R_c plot and the pressure, density and particle velocity profiles just described we can

conclude that Porzel's method is by far the superior of all the non-similar analytical techniques and yields an adequate description of the dynamics and flow structure of reacting blasts for the entire regime of propagation, i.e., $0 \leq \eta' \leq 1$.

4. The Asymptotic Regime

In their analysis of the asymptotic decay of a reacting blast wave to its C-J state, Levin and Chernyi [5] obtained an expression for the shock decay coefficient $\theta = R_s \ddot{R}_s / \dot{R}_s^2$ by evaluating the three conservation equations at the front $\xi = 1$ and then taking the limit as $M_s \to M_{CJ}$ or $\epsilon = 1-\eta' = 1 - M_{CJ}^2/M_s^2 \to 0$, i.e.,

$$\theta = -K_1 \epsilon^{\frac{1}{2}} - K_2 \epsilon \tag{4.1}$$

where

$$K_1 = \frac{j(\gamma + \eta_{cj})}{2(\gamma + 1)} \left(\frac{1 - \eta_{cj}}{1 + \eta_{cj}} \right)^{\frac{1}{2}} \tag{4.2}$$

and

$$K_2 = \frac{\gamma + 1}{2} \left. \frac{d\phi}{d\xi} \right|_{\substack{\xi = 1 \\ \epsilon \to 0}} \tag{4.3}$$

The numerical constant $j = 0, 1, 2$ for planar, cylindrical and spherical waves respectively and $\eta_{CJ} = 1/M_{CJ}^2$. Levin and Chernyi then assumed that the blast wave solution recovers

the J-T-Z similarity solution in the limit as $\varepsilon \to 0$, hence

$$\left.\frac{d\phi}{d\xi}\right|_{\substack{\xi=1\\ \epsilon\to 0}} \longrightarrow \infty \qquad like \quad (1-\xi)^{-\frac{1}{2}}$$

By further assuming that the particle velocity gradient approaches infinity as $\varepsilon \to 0$ like $\varepsilon^{-\frac{1}{2}}$, one notes that $K_2 \to \infty$ like $\varepsilon^{-\frac{1}{2}}$ as $\varepsilon \to 0$ and Eq. 4.1 yields in the limit as $\varepsilon \to 0$ for $j \neq 0$ the following relationship:

$$\theta = C\,\epsilon^{1/2} \tag{4.4}$$

where C is some arbitrary constant. For the planar case where $j = 0$, one notes from Eq. 4.2 that $K_1 = 0$ and as $\varepsilon \to 0$, the J-T-Z solution yields

$$\left.\frac{d\phi}{d\xi}\right|_{\substack{\xi=1\\ \epsilon\to 0}} \longrightarrow \frac{2}{\gamma+1}$$

Hence $K_2 \to 1$ as $\varepsilon \to 0$ for the planar case and Eq. 4.1 becomes in the limit as $\varepsilon \to 0$,

$$\theta = -\epsilon \tag{4.5}$$

From the definition of θ, one notes that

$$\theta = -\frac{2R_S}{\eta'}\frac{d\eta'}{dR_S} \simeq -2R_S\frac{d\eta'}{dR_S} = 2R_S\frac{d\epsilon}{dR_S} \tag{4.6}$$

since $\eta' \simeq 1$ as $\varepsilon \to 0$. Using the above equation and Eq. 4.5 for $j = 0$ and Eq. 4.4 for $j \neq 0$, one gets the following results

for the asymptotic decay:

$$\epsilon = 1 - \eta' = \left(\frac{R_{so}}{R_s} \right)^2 \quad for \quad j = 0 \qquad (4.7)$$

$$\epsilon^{\frac{j}{2}} = \epsilon_0^{\frac{j}{2}} - C' \ln \frac{R_s}{R_{so}} \qquad for \quad j \neq 0 \qquad (4.8)$$

where R_{so}, ϵ_0, and C' are arbitrary integration constants. From Eq. 4.7 it is evident that for planar waves, the decay to the C-J state is asymptotic with $R_s \to \infty$ as $\epsilon \to 0$. However, from Eq. 4.8, one notes that in the limit as $\epsilon \to 0$, $R_s \to R_{CJ}$ which is finite and given as

$$(R_s)_{\epsilon \to 0} = R_{CJ} = R_{so} \exp \left(\frac{\epsilon_0^{\frac{j}{2}}}{C'} \right) \qquad (4.9)$$

The present numerical solution confirms the conclusion of Levin and Chernyi that the decay to the C-J state is achieved at a finite radius for diverging waves (i.e., $j = 1, 2$). From the present numerical solution the value of R_{CJ} for various values of γ and M_{CJ} are shown in Fig. 5. Here R_{CJ} is calculated from:

a) the present numerical solution

b) Levin and Chernyi's asymptotic formula

c) an asymptotic formula newly derived in the present paper

d) values quoted by Chernyi, Korobeinikov et al [10] for three chosen values of M_{CJ} which characterize the mixture and for various values of γ.

To check the asymptotic formula of Levin and Chernyi, the arbitrary constants R_{so}, ε_o and C' in Eq. 4.9 are evaluated by matching Eq. 4.8, at some finite but small value of ε (typically $\varepsilon \simeq 1-\eta' \simeq .05$ for $\eta' \simeq .95$), with both the present numerical solution and also the analytical solution using Porzel's method. With the constants thus determined, Levin and Chernyi's values of R_{CJ} found from Eq. 4.9 agree well with those from the exact numerical solution. Also shown in Fig. 5 are the values of R_{CJ} quoted by Chernyi, Korobeinikov et al [8]. Again, good agreement with the present exact numerical solution is obtained. The discrepancies that do exist are due to the choice of R_{so} or η'_o (or ε_o). If one chooses ε_o closer to zero (i.e., $M_s \simeq M_{CJ}$) the values of R_{CJ} obtained from the asymptotic formulae will agree even better with the exact values from the numerical solution. Hence we conclude that the asymptotic formula given by Levin and Chernyi predicts correctly the value of R_{CJ}. However, from the present numerical solution, it can be observed from Fig. 4 that the particle velocity profile as $\varepsilon \to 0$ does not recover the J-T-Z similarity solution. The gradient at the front as $\varepsilon \to 0$ remains finite instead of approaching infinity as predicted by the J-T-Z solution. The value of the velocity gradient from the present exact solution is found to approach that of the planar case instead, i.e.,

$$\left.\frac{d\phi}{d\xi}\right|_{\substack{\xi=1\\ \epsilon\to 0}} \longrightarrow \frac{2}{\gamma+1} \tag{4.10}$$

From a physical point of view this result is quite plausible since as the spherical wave expands, curvature effects become progressively unimportant. At large shock radii, diverging waves must become essentially planar when curvature efforts are negligible.

The fact that Levin and Chernyi's formula predicts the same value for R_{CJ} as the present numerical solution even though the numerical solution yields a totally different value for the velocity gradient in the limit as $R_s \to R_{CJ}$ requires clarification. Instead of assuming that the J-T-Z solution is recovered as $\varepsilon \to 0$ with the result that $\left.\frac{d\phi}{d\xi}\right|_{\substack{\xi=1 \\ \varepsilon\to 0}} \to \infty$, we take the particle velocity gradient to approach a finite constant α as indicated by the present numerical solution. Hence from Eq. 4.3 we see that $K_2 \to \frac{\gamma+1}{2}\alpha$ as $\varepsilon \to 0$. From Eq. 4.1 and Eq. 4.6, we obtain

$$\int_{R_{so}}^{R_{CJ}} \frac{dR_s}{R_s} = -\int_{\epsilon_0}^{0} \frac{d\epsilon}{2(K_1\epsilon^{1/2} + K_2\epsilon)}$$

and carrying out the integration leads to the following asymptotic law instead of that given by Levin and Chernyi (i.e., Eq. 4.8):

$$R_s = R_{so}\left(\frac{1 + \frac{K_2}{K_1}\epsilon_0^{1/2}}{1 + \frac{K_2}{K_1}\epsilon^{1/2}}\right)^{\frac{1}{K_2}} \tag{4.11}$$

In the limit as $\varepsilon \to 0$ and $R_s \to R_{CJ}$ we get

$$R_{CJ} = R_{SO} \left(1 + \frac{K_2}{K_1} \epsilon_0^{1/2} \right)^{\frac{1}{K_2}} \tag{4.12}$$

instead of Eq. 4.9 as given by Levin and Chernyi. In the present asymptotic law, we find first that for the planar case, $j = 0$ and Eq. 4.2 yields $K_1 = 0$. Hence Eq. 4.12 yields $R_{CJ} \to \infty$ as $\varepsilon \to 0$ as predicted by Levin and Chernyi. In arriving at this result from our asymptotic law note that it is not necessary to assume that the J-T-Z solution is recovered in the limit as $\varepsilon \to 0$ as is required in Levin and Chernyi's analysis. By expanding Eq. 4.12, we obtain

$$R_{CJ} = R_{SO} \left(1 + \frac{1}{K_1} \epsilon_0^{1/2} \right) \tag{4.13}$$

up to the order of $\varepsilon_0^{\frac{1}{2}}$. From Eq. 4.13, we see therefore that R_{CJ} is independent on K_2, hence independent of the particle velocity gradient. This independence of R_{CJ} on $\left.\frac{d\phi}{d\xi}\right|_{\substack{\xi=1 \\ \varepsilon\to 0}}$ implies that it is irrelevant whether the J-T-Z solution is recovered or not in the limit as $\varepsilon \to 0$. If we approach the exponential term in Levin and Chernyi's formula given by Eq. 4.9 we see that it is identical to Eq. 4.13 to the order of $\varepsilon_0^{\frac{1}{2}}$. This explains why identical results for k_{CJ} are obtained using Eq. 4.9 and from the present numerical solution even though the numerical solution does not approach the J-T-Z similarity solution as $\varepsilon \to 0$. The present solution indicates that the particle velocity

gradient at the front approaches that of the planar case (i.e., Eq. 4.10), hence $K_2 = 1$. The values of R_{CJ} computed from Eq. 4.13 using $K_2 = 1$ yield values much closer to the exact ones than the Levin and Chernyi formula even though the same value of ε_0 is used to evaluate the constants in the asymptotic formulae.

The range of validity of the asymptotic formula (i.e., Eq. 4.11 with $K_2 = 1$) can be seen from Fig. 6 where the shock decay coefficient θ is plotted against the shock strength $\eta' = (M_{CJ}/M_s)^2$. For the range $.6 \lesssim \eta' \leq 1$ the asymptotic law yields almost identical results to the exact numerical solution. In other words, the decay from moderate strengths to the final C-J state is adequately described by the asymptotic formulae. Hence as far as the decay of the reacting blast is concerned the asymptotic formula coupled with an analytical solution such as the solution using Porzel's method can provide a good description of the entire decay process from $\eta' = 0$ to $\eta' = 1$.

It is also interesting to note from Fig. 5 that a decaying reacting blast approaches the C-J state in less than an explosion length R_0 for most gaseous explosives with the range $5 \leq M_{CJ} \lesssim 10$ and $\gamma \simeq 1.3$. From previous experiments on direct initiation of C_2H_2-O_2 mixtures, the critical energy for direct initiation is of the order of 0.3 joules for stoicniometric mixtures at an initial pressure of 100 torr. The explosive length for this case is of the order of 1 cm. Hence the C-J state is reached when the blast radius is of the order of 0.7 cm. This makes experimental verification of the

early time regime in which the reacting blast solutions are valid extremely difficult, and existing measurements of the shock parameters are mostly limited to the asymptotic regime.

5. The Finite Kinetic Rate (F-K-R) Solution

For the numerical solution of the double front F-K-R model, the empirical relationships for the induction time are taken from White [30]

$$\log\left(\tau_i \cdot [O_2]^{\frac{1}{3}} \cdot [C_2H_2]^{\frac{2}{3}}\right) = -10.81 + \frac{17,300}{4.58\,T} \qquad (5.1)$$

Strehlow [24]

$$\log\left(\tau_i \cdot [O_2]\right) = -10.269 + \frac{17,153}{4.58\,T} \qquad (5.2)$$

and Strehlow and Engel [31]

$$\log\left(\tau_i \cdot [O_2]\right) = -10.56 + \frac{17,060}{4.58\,T} \qquad (5.3)$$

To illustrate the typical numerical results, the particular case of stoichiometric acetylene-oxygen mixture at an initial pressure of 100 torr is chosen. Fig. 7 shows the variation of the shock Mach number with shock radius for various values of the initiation energy E_0. For a given initiation energy E_0, the initial decay is similar to that of the R-B-W solution which assumes the reaction rates to be infinite. This is to be expected since in the early time regime the shock is very

strong, hence the induction distance is sufficiently small for the discontinuity assumption to be valid. As the blast expands and weakens the reaction zone progressively lags behind. From Fig. 7 we note that the shock decays past the C-J state for the particular mixture whereupon a quasi-steady state is reached when the shock and reaction front complex propagate at a constant sub C-J velocity. The existence of this quasi-steady regime of propagation has been confirmed experimentally by Soloukhin [32], Bach, Knystautas and Lee [22], Struck [9] and Brossard [11]. The present solution also confirms the existence of a critical energy for direct initiation. From Fig. 7 we note that for $E_0 < .001$ joules, the quasi-steady regime cannot be obtained. The shock decays continuously to the acoustic limit and the trailing reaction front completely decouples from the shock and continues to propagate as a spherical flame. This sub-critical energy regime of propagation has been studied previously by the Authors [22] on laser spark generated spherical detonations. The present numerical solution breaks down, marking the termination of the quasi-steady regime after a finite period of time. This is due to the fact that sharp gradients are developed in the flow field behind the reaction-shock front complex during this quasi-steady regime. The development of these sharp gradients in pressure, density and particle velocity in the flow field are illustrated in Figs. 8 to 10. It is to be noted that these sharp gradients are not a result of the stability of the numerical scheme used. Rather, it is a physical phenomenon that occurs whenever a shock wave is

supported solely by chemical reactions that occur at a finite rate. Other numerical studies of the propagation of exothermic shock waves [33, 24] also demonstrate the onset of oscillations and instability under the critical conditions when the shock is mainly supported by the energy released due to combustion. Experimentally it is found that the termination of the quasi-steady regime is marked by the sudden violent transition to a multiheaded spherical detonation wave [22]. Therefore as far as qualitative features are concerned the present numerical solution confirms existing experimental observations of spherical detonation phenomena.

A quantitative comparison between the present solution and experimental results for the shock and reaction front trajectories are shown in Figs. 11 and 12. In Fig. 11, the stoichiometric C_2H_2-O_2 mixture is diluted by 70% inert N_2. Initiation is by laser spark with spark energy E_0 = 0.3 joules. This corresponds to the sub-critical regime where the shock and reaction front progressively decouple from each other. In Fig. 12, the mixture is undiluted and the same initiation energy E_0 = 0.3 joules corresponds to the critical energy for direct initiation. Experimentally it is observed that decoupling of the shock and reaction front is followed by a quasi-steady regime at the termination of which is the re-establishment to a highly asymmetrical multiheaded spherical detonation. Photographic records of these two cases are given in a previous paper [22]. From Figs. 11 and 12 we can see that the present solution agrees

quite well with experiments as far as shock and reaction trajectories are concerned.

For the same experimental conditions as Fig. 11, the induction times for each particle crossing the blast wave at different initial radii are measured from the experimental records. A comparison with the results from the present solution indicates fairly good agreement (Fig. 13). Also shown in Fig. 11 are the results obtained from an analytical solution based on Porzel's method where it is assumed that the energy released by chemical reaction has a negligible influence on the hydrodynamic flow structure. The importance of the chemical energy in perturbing the non-reacting blast flow structure even in this case of 70% inert nitrogen dilution is self-evident.

From the present solution it is also possible to determine the critical energy for direct initiation for a given mixture at given initial conditions. The particular case for stoichiometric C_2H_2-O_2 mixtures is shown in Fig. 14. The experimental results are based on the laser spark as an energy source. The small range in experimental data is due to the limited power range of the ruby laser used. The theoretical prediction of the limiting critical energy based on the numerical solution of the F-K-R model yields values which are considerably lower than the experimental results using the laser spark from the Q-switched ruby laser. Of all the experimental initiation results currently available those with the laser spark from the Q-switched system, apart from

being the most extensively available, represented the shortest deposition times (∿ nanoseconds) and hence were felt to be the ones most appropriate for comparison in view of the theoretical premise of vanishing pulse length. We attribute the discrepancy to two possible causes. The first is that approximate global kinetic data are used in the theoretical calculations. Moreover, such calculations indicate that the solution is very sensitive to the specific values of the empirical constants used in the global induction time relations among which there exist significant discrepancies depending on the source quoting the relationship. The second possible source of disagreement is that strictly speaking the laser spark from a Q-switched ruby system does not simulate ideally the limiting value of source energy (i.e., not infinite power since pulse duration ∿ 20 nanoseconds). More reliable conclusions in this regard have to await initiation experiments with sub-nanosecond laser sparks which would simulate the infinite source power and hence the limiting source energy criterion more closely. We are currently initiating such experiments.

6. Prediction of Transverse Wave Spacings

The cellular dimension in a multiheaded detonation front is an important characteristic of the explosive system and its initial conditions. A recent theoretical attempt has been made by Strehlow [34] to predict the cellular dimension or the transverse wave spacing. Detailed experimental observations [2]

of the motion of a "detonation wavelet" in between collisions of transverse waves indicates that it behaves like a decaying reactive blast wave. The minimum strength of a detonation wavelet just prior to the explosive re-energization by the collision of a pair of transverse waves is found to be of the order of $M_s \simeq 3$. From Fig. 7 we note that the minimum shock strength which corresponds to an initiation energy equal to the critical value is also of the order of 3. For any initiation energy less than the critical value the shock decays to the acoustic limit. Hence if we assume that the energy released in the collision of a pair of transverse waves corresponds to the critical value we can make a formal analogy and take the shock radius when M_s is a minimum as the longitudinal dimension of the detonation cell. Using the present numerical solution, it is then possible to evaluate the dimension of a detonation cell based on the above reasoning. A comparison between the theoretically predicted values with the experimental data of Strehlow[31] for argon diluted C_2H_2-O_2, H_2-O_2, and C_2H_4-O_2 mixtures are shown in Figs. 15 to 17 respectively. The predictions of the transverse wave dimensions made in this way based on the present numerical solution of the F-K-R model are in rough agreement with experimental measurements of Strehlow[31]. Once again the discrepancies can possibly be attributed to the global approximate kinetic rate assumption used in the numerical solution and the oversimplified representation of the re-energization of "detonation wavelets" upon mutual transverse

collision by a point energy source of infinite power density. It has been pointed out by Strehlow that the blast wave model for transverse wave spacing can at best be used in a qualitative sense since the energy released by the collision of transverse waves is not instantaneous as assumed in the theoretical model, and also from experiments it is found that the center of the curved detonation wavelet does not correspond to the point where the transverse waves collide. However, in view of the fair agreement between the theoretical results and experimental data we conclude that the blast wave model can be used to provide an a-priori prediction of the transverse wave spacings at present until better theoretical models are developed. It is to be noted that the fundamental mechanisms for the propagation of multiheaded detonation waves remain obscure, and the present blast wave model fails to throw light on why nature prefers detonative combustion to proceed in such a complex manner although the model does predict the cellular dimensions themselves.

7. Conclusions

Using the present exact numerical solution as a reference for comparison, it is found that Porzel's method of the power law density profile gives the most accurate description of the motion of a reacting blast wave with the widest range of applicability. In the asymptotic regime as the blast approaches the C-J state, the present solution

confirms the results of Levin and Chernyi in that for diverging waves, the C-J state is reached at a finite radius. Although the asymptotic law given by Levin and Chernyi does give the correct prediction of the C-J radius, the assumption they invoke that the J-T-Z similarity is recovered in the limit $\varepsilon \to 0$ is not supported by the present results. Instead the present solution indicates that the solution approaches the planar case in the limit with all the flow gradients behind the front being finite. To resolve this inconsistency, a new asymptotic decay law is developed based on finite flow gradients behind the shock as the C-J state is reached. The present asymptotic formula shows that to the order of $\varepsilon^{\frac{1}{2}}$, the C-J radius is independent of the flow gradient and hence explains why the formula of Levin and Chernyi yields the correct value of R_{CJ} while differing in the assumption as to the nature of the flow gradient used in the analysis. Comparing with the exact numerical solution it is found that the asymptotic decay law is valid for a wide range of shock strengths. Coupled with an analytical solution for the initial early time propagation regime, the entire decay of a reacting blast can be described quite accurately. The finite kinetic rate solution is found not only to predict all the essential qualitative features of the propagation of a spherical combustion wave but predicts quantitatively the shock and reaction front trajectories and the critical energy regime for direct initiation. Using a blast wave model for cellular detonations the theoretically predicted values of the transverse wave spacings are found to be

in fair agreement with the experimental data of Strehlow.

8. References

1. LEE, J.H. — "The Propagation of Shocks and Blast Waves in a Detonating Gas" Mech. Eng. Research Lab. Report 65-1, McGill University (1965).

2. LEE, J.H., SOLOUKHIN, R.I. and Oppenheim, A.K. — "Current Views on Gaseous Detonation" Astronautica Acta 14, 565-582 (1969).

3. LEE, J.H., KNYSTAUTAS, R. and BACH, G.G. — "Theory of Explosions" Mech. Eng. Research Lab. Report 69-10; also US AFOSR 69-3090TR (1969).

4. KOROBEINIKOV, V. — "Gasdynamics of Explosions" Ann. Rev. Fluid Mech. 3, 317-346 (1971).

5. CHERNYI, G.G. and LEVIN, V.A. — "Asymptotic Laws of Behavior of Detonation Waves" P.M.M. 31, 393-405 (1967).

6. LUNDSTROM, G.A. and OPPENHEIM, A.K. — "On the Influence of Non-Steadiness on the Thickness of the Detonation Wave" Proc. Roy. Soc. A310, 463-478 (1969).

7. KOROBEINIKOV, V. — "The Problem of Point Explosion in a Detonating Gas" Astronautica Acta 14, 411-419 (1969).

8. CHERNYI, G.G. and MEDVEDEV, S.A. — "Development of Oscillations Associated with the Attenuation of Detonation Waves" Astronautica Acta 15, 371-375 (1970).

9. STRUCK, W. — "Kugelformige Detonationswellen in Gasgemischen" Dissertation, Techn. University of Aachen (1968).

10. BISHIMOV, E., KOROBEINIKOV, V. and LEVIN, V. — "Strong Explosion in Combustible Gaseous Mixture" Astronautica Acta 15, 267-273 (1970).

11. BROSSARD, J. "Contribution a l'etude des ondes de choc et de combustion spherique divergentes dans les gaz" These de doctorat, Universite de Poitiers (1970).

12. CHERET, R. "Sur la nature singuliere du couplage entre ecoulement et reactions chimiques dans l'onde explosive ideale" Comptes Rendus 269B, 603-606 (1969).

13. BACH, G.G. and LEE, J.H. "On the Propagation of Spherical Detonation Waves" Mech. Eng. Research Lab. Report 72-9 (1972).

14. TAYLOR, G.I. "The Formation of a Blast Wave by Very Intense Explosion. I. Theoretical Discussion" Proc. Roy. Soc. 201A, 159-164 (1950).

15. SEDOV, L.I. "Similarity and Dimensional Methods in Mechanics" Academic Press Inc., New York, 1959.

16. OSHIMA, K. "Blast Waves Produced by Exploding Wire" Aero. Res. Inst. Rep. No. 358, University of Tokyo (1960).

17. SAKURAI, A. "On the Propagation and Structure of the Blast Wave"
Part I: Jour. Phys. Soc. Japan 8, 662-669 (1953)
Part II: Jour. Phys. Soc. Japan 9, 256-266 (1954).

18. PORZEL, F.B. "Height of Burse for Atomic Bomb - I; The Free Air Curve" Rept. LA-1664, Los Alamos Scientific Lab. (1954).

19. JOUGUET, M. "La Mecanique des Explosifs" 359-366 (Ed. by Doin) Paris (1917).

20. TAYLOR, G.I. "The Dynamics of the Combustion Products behind Plane and Spherical Detonation Fronts in Explosives" Proc. Roy. Soc. A200, 235-247 (1950).

21. ZELDOVICH, Ya.B. "Distribution of Pressure and Velocity in the Products of a Detonating Explosion, and in Particular in the Case of a Spherical Propagation of the Detonation Waves" J. Exp. Theor. Phys. (USSR) 12. 389-406 (1942).

22. BACH, G.G., KNYSTAUTAS, R. and LEE, J.H. "Direct Initiation of Spherical Detonations in Gaseous Explosives" Proc. 12th Symp. (Int.) Combustion, Poitiers (1968); Combustion Institute, Pittsburgh, 853-864 (1969).

23. BACH, G.G., GUIRAO, C., KNYSTAUTAS, R., LEE, J.H. and ALCOCK, J. "The Laser Spark for Gas Kinetic Studies" Proc. 8th Int. Shock Tube Symp., London (1971); Chapman and Hall, London, 34/1-34/12 (1971).

24. STREHLOW, R.A., CROOKER, A.J. and CASEY, R.E. "Detonation Initiation Behind an Accelerating Shock Wave" Comb. and Flame 11, 334-351 (1967).

25. CHOU, P.C. and HUANG, S.L. "Calculation of Expanding Shock Waves and Late-Stage Equivalence" Drexel Institute of Technology Rept. 125-12 (1968).

26. RAE, W.J. "Non-Similar Solutions for Impact Generated Shock Propagation in Solids" Cornell Aero. Lab. Rep. AI-1821-A-2, NASA CR-54251, March 1965.

27. BACH, G.G. and LEE, J.H. "An Analytical Solution for Blast Waves" AIAA Jour. 8, 271-275 (1970).

28. LEE, J.H., LEE, B.H.K. and SHANFIELD, I. "Two-Dimensional Unconfined Gaseous Detonation Waves" Proc. 10th Symp. (Int.) Combustion, Cambridge (1964); The Combustion Institute, Pittsburgh, 805-815 (1965).

29. BACH, G.G., KNYSTAUTAS, R. and LEE, J.H. "Initiation Criteria for Diverging Gaseous Detonations" Proc. 13th Symp. (Int.) Combustion, Salt Lake City, Utah, August 1970; Comb. Inst., Pittsburgh, Pa., 1097-1110 (1971).

30. WHITE, D.R. "Density Induction Times in Very Lean Mixtures of D_2, H_2, C_2H_2 and C_2H_4 with O_2" Proc. 11th Symp. (Int.) Combustion, Berkeley, 1966; Comb. Inst., Pittsburgh, Pa., 147-154 (1967).

31. STREHLOW, R.A. and ENGEL, C.D. "Transverse Waves in Detonations: II. Structure and Spacing in H_2-O_2, C_2H_2-O_2, C_2H_4-O_2 and CH_4-O_2 Systems" AIAA Jour. 7, 492 (1969).

32. SOLOUKHIN, R.I. "Quasi-Stationary Reaction Zone in Gaseous Detonation" Proc. 11th Symp. (Int.) Combustion, Berkeley, 1966; Comb. Inst., Pittsburgh, Pa., 671-676 (1967).

33. FICKETT, W. and WOOD, W.W. "Flow Calculations for Pulsating One-Dimensional Detonations" Phys. Fluids 9, 903 (1966).

34. STREHLOW, R.A. "Fundamentals of Combustion" International Textbook Co., Scranton, Pa. (1968).

9. Acknowledgements

This research was performed under the auspices of US AFOSR continuing Grant AFOSR 69-1752B and by the National Research Council of Canada under Grants A-118, A-3347 and A-7091. One of us (J.H. Lee) is grateful to the Academy of Sciences (USSR) and the National Research Council of Canada for the opportunity to visit the Steklov Mathematical Institute where numerous discussions with Drs. V.P. Korobeinikov and V.A. Levin helped to clarify a number of issues on the subject, particularly on the motion of detonation waves.

10. Figure Captions

Fig. 1 Comparison of the variation of shock strength η' with shock radius R_s/R_o for spherical detonation waves, $\gamma = 1.4$, $M_{CJ} = 7.0501$ from the various analytical solutions with the numerical exact solution.

Fig. 2 Comparison of pressure profiles behind the reacting blast wave for various blast radii.

Fig. 3 Comparison of density profiles behind the reacting blast waves for various blast radii.

Fig. 4 Comparison of particle velocity profiles behind the reacting blast wave for various blast radii.

Fig. 5 Comparison of the values of finite C-J radius R_{CJ}/R_o for various values of γ and M_{CJ}.

Fig. 6 Variation of shock decay coefficient θ with shock strength.

Fig. 7 Variation of shock Mach number with shock radius for spherical detonation waves corresponding to different source energies.

Fig. 8 Pressure profiles for a spherical detonation wave with critical initiation energy (stoichiometric C_2H_2-O_2, $E_o = .001J$, $P_o = 100mmHg$).

Fig. 9 Density profiles for a spherical detonation wave with critical initiation energy (stoichiometric C_2H_2-O_2, E_o = .001J, P_o = 100mmHg).

Fig. 10 Particle velocity profiles for a spherical detonation wave with critical initiation energy (stoichiometric C_2H_2-O_2, E_o = .001J, P_o = 100mmHg).

Fig. 11 Spherical shock and reaction front trajectories in a detonable mixture with sub-critical initiation energy $(0.3(\frac{2}{7}C_2H_2+\frac{5}{7}O_2)+0.7N_2$, E_o = .3J, P_o = 100mmHg).

Fig. 12 Spherical shock and reaction front trajectories in a detonable mixture (stoichiometric C_2H_2-O_2, E_o = .3J, P_o = 100mmHg).

Fig. 13 The induction period for particles crossing a spherical blast wave at different shock Mach numbers.

Fig. 14 Comparison between theoretical predictions and experimental results of critical initiation energies (stoichiometric C_2H_2-O_2).

Fig. 15, Fig. 16, Fig. 17 Variation of transverse wave spacings of spherical detonation waves with initial pressure of mixtures (C_2H_2-O_2-Ar, H_2-O_2-Ar and C_2H_4-O_2-Ar respectively).

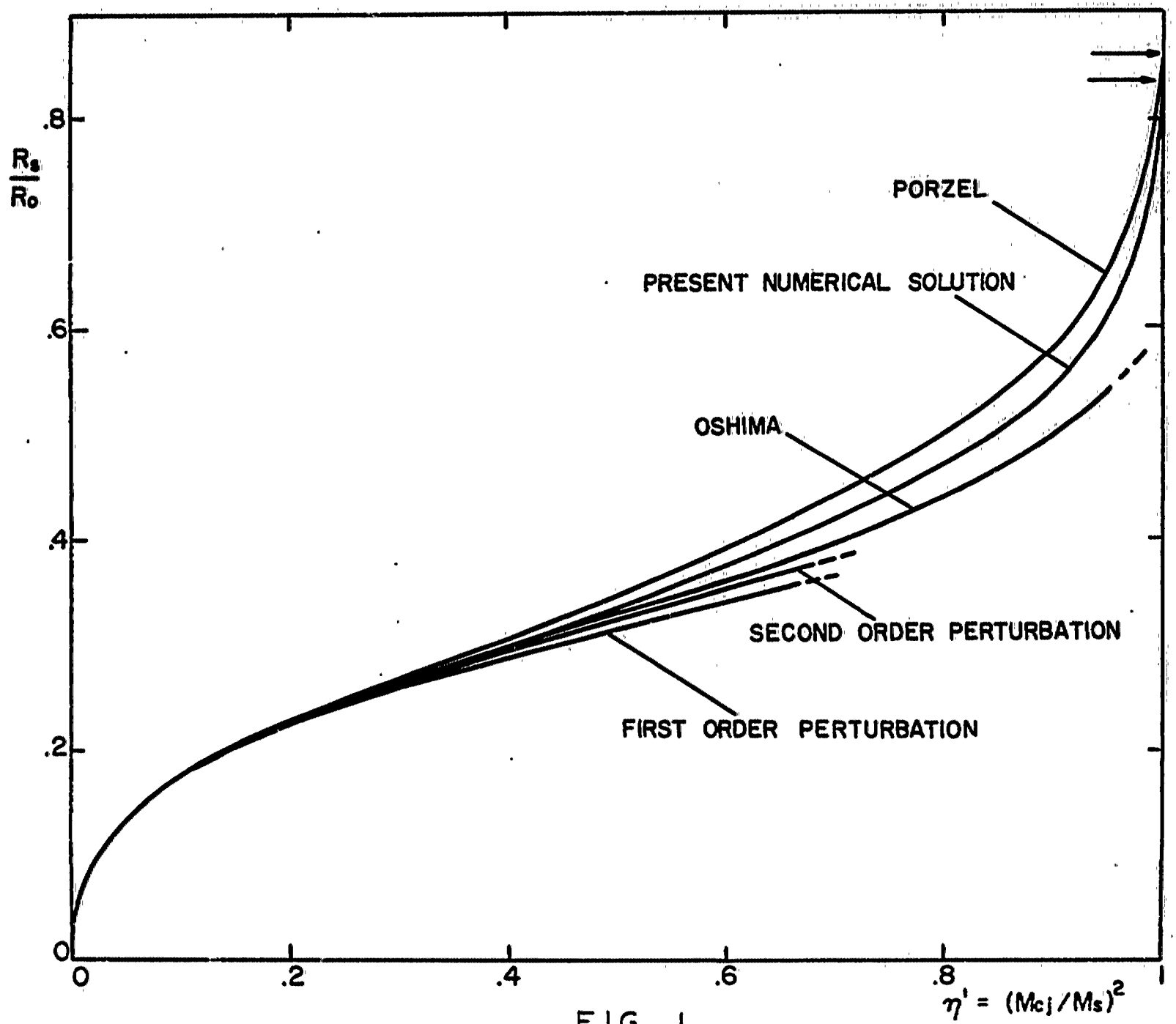
$\frac{R_s}{R_o}$
.8
.6
.4
.2
0
0
.2
.4
.6
.8
1
$\eta' = (M_{cj}/M_s)^2$
PORZEL
PRESENT NUMERICAL SOLUTION
OSHIMA
SECOND ORDER PERTURBATION
FIRST ORDER PERTURBATION

FIG. 1

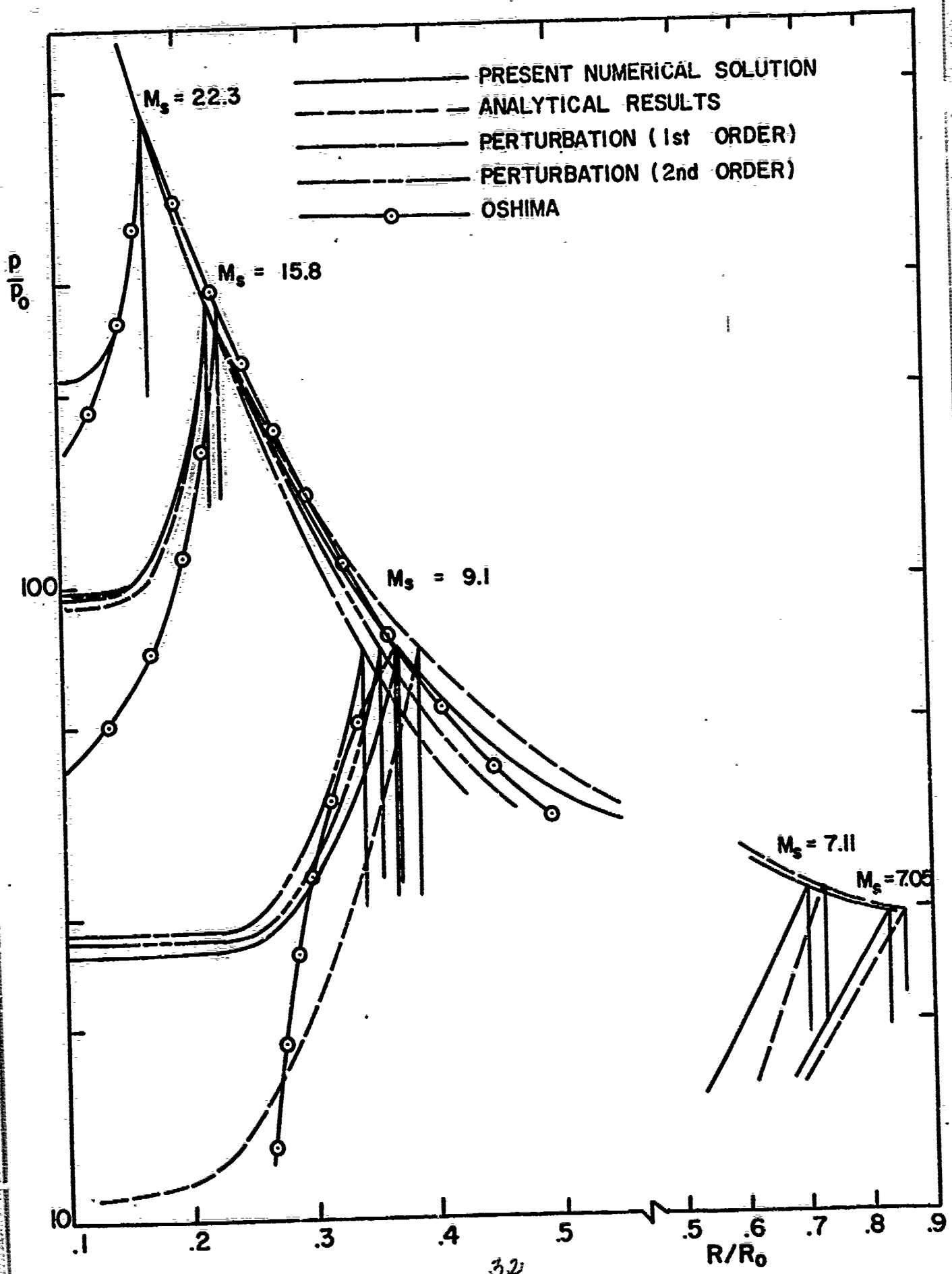
PRESENT NUMERICAL SOLUTION
ANALYTICAL RESULTS
PERTURBATION (1st ORDER)
PERTURBATION (2nd ORDER)
OSHIMA
$M_s = 22.3$
$M_s = 15.8$
$M_s = 9.1$
$M_s = 7.11$
$M_s = 7.05$
$\frac{p}{p_0}$
100
10
.1
.2
.3
.4
.5
.5
.6
.7
.8
.9
R/R_0

FIG. 2

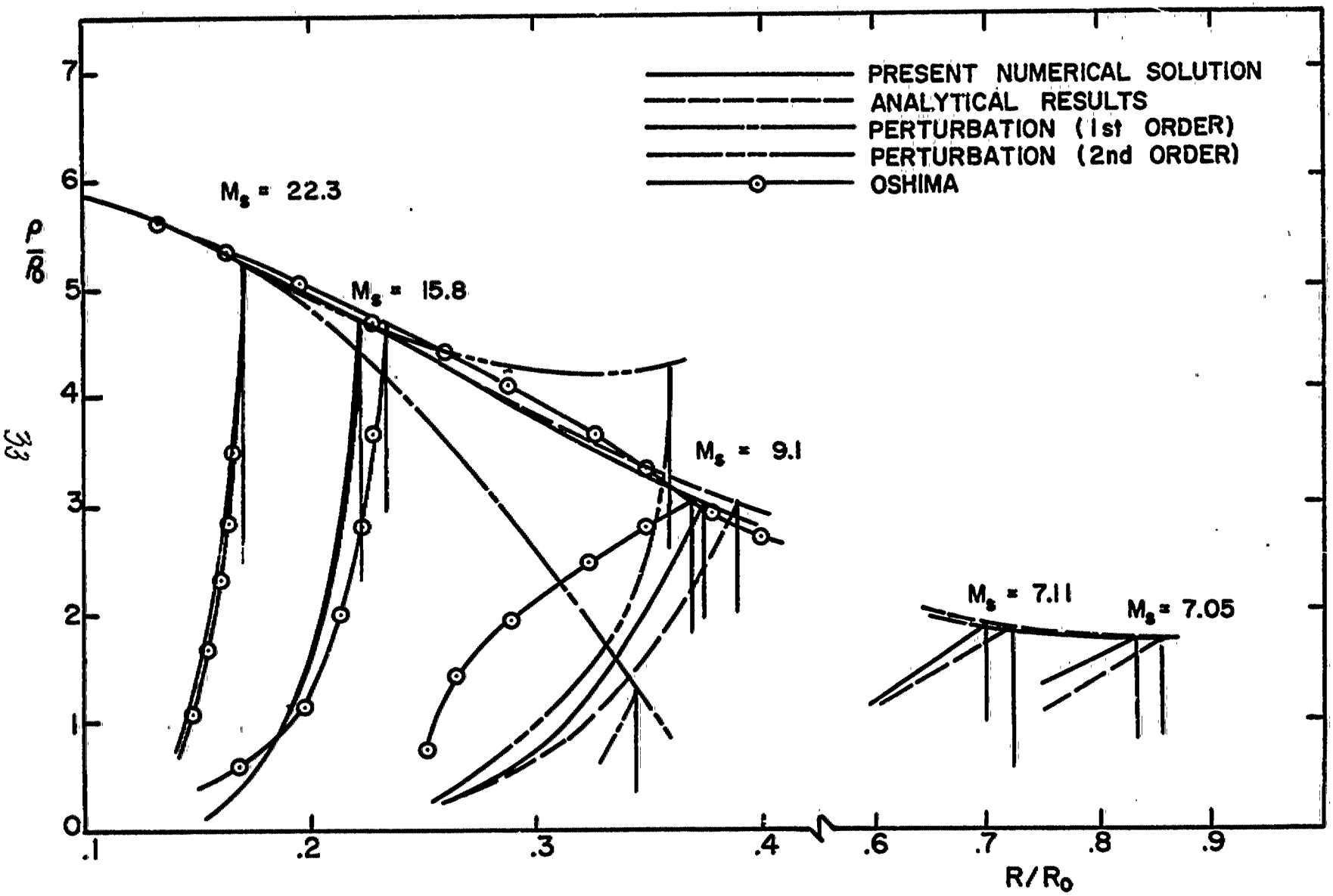
PRESENT NUMERICAL SOLUTION
ANALYTICAL RESULTS
PERTURBATION (1st ORDER)
PERTURBATION (2nd ORDER)
OSHIMA
M_s = 22.3
M_s = 15.8
M_s = 9.1
M_s = 7.11
M_s = 7.05
$\rho/\bar{\rho}_0$
R/R_0
0
1
2
3
4
5
6
7
.1
.2
.3
.4
.6
.7
.8
.9

FIG. 3

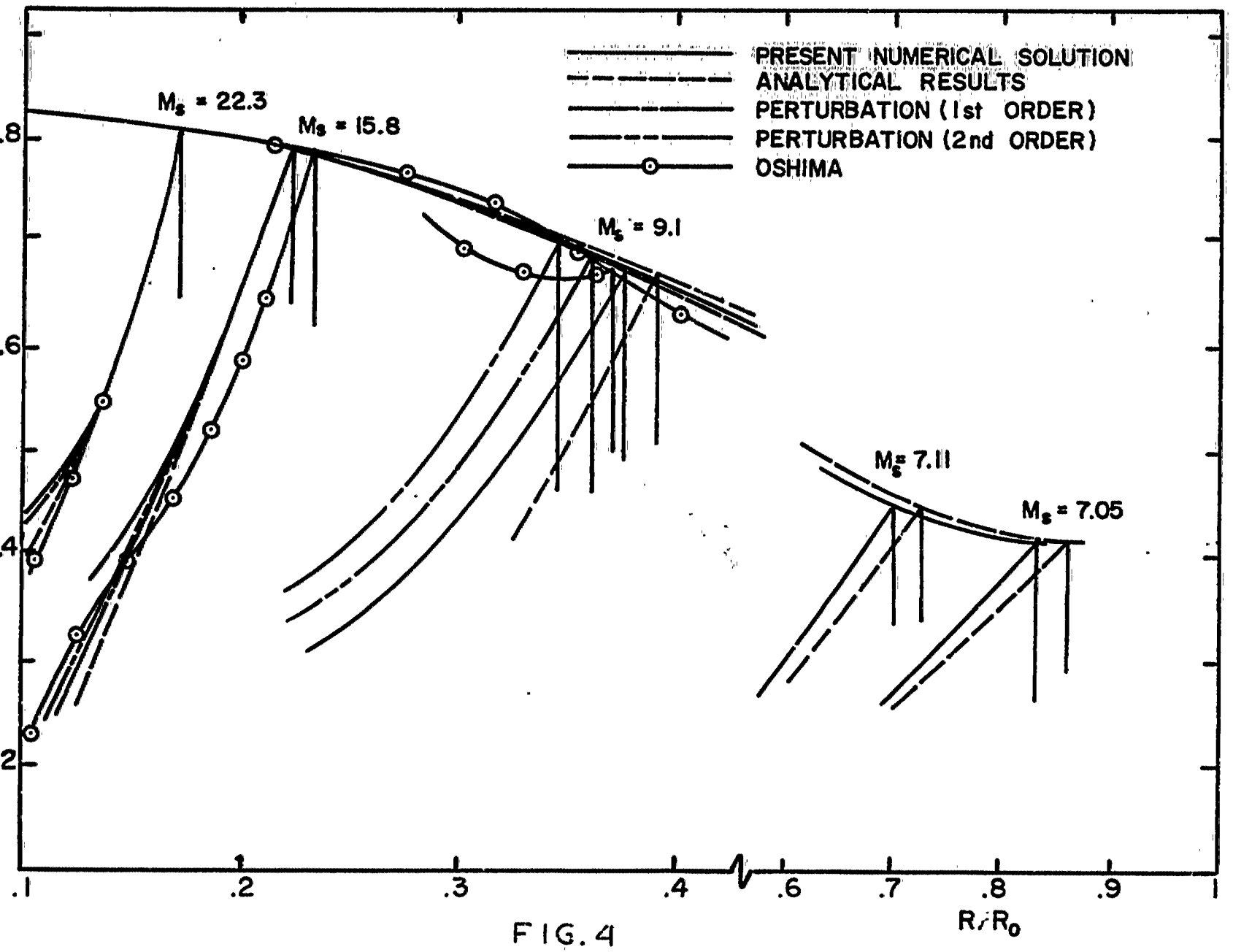
PRESENT NUMERICAL SOLUTION
ANALYTICAL RESULTS
PERTURBATION (1st ORDER)
PERTURBATION (2nd ORDER)
OSHIMA
M_s = 22.3
M_s = 15.8
M_s = 9.1
M_s = 7.11
M_s = 7.05
$\frac{u}{\dot{R}_s}$
.8
.6
.4
.2
.1
.2
.3
.4
.6
.7
.8
.9
1
R/R_0

FIG. 4

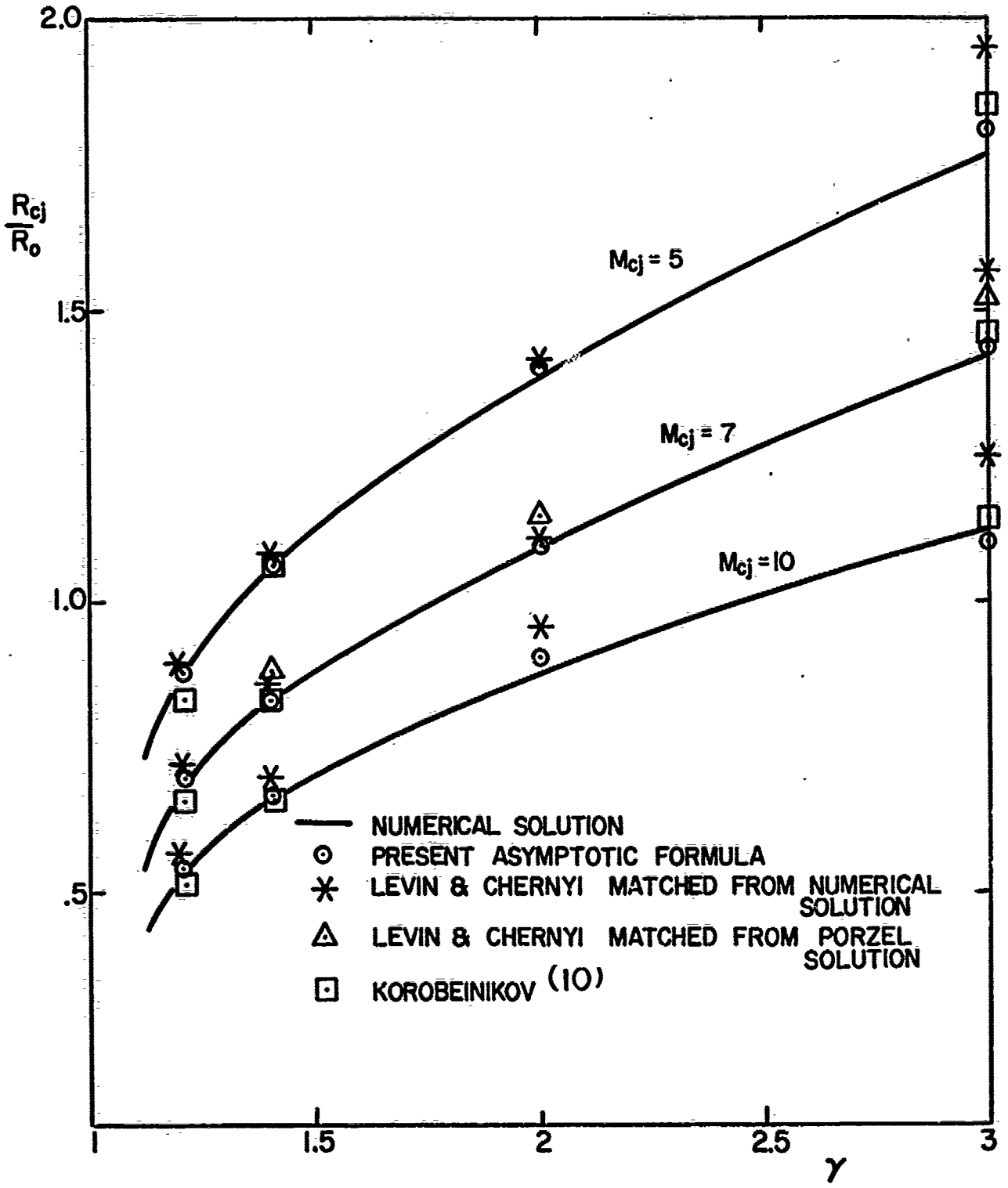
2.0
1.5
1.0
.5
$\frac{R_{cj}}{R_o}$
$M_{cj} = 5$
$M_{cj} = 7$
$M_{cj} = 10$
NUMERICAL SOLUTION
PRESENT ASYMPTOTIC FORMULA
LEVIN & CHERNYI MATCHED FROM NUMERICAL SOLUTION
LEVIN & CHERNYI MATCHED FROM PORZEL SOLUTION
KOROBEINIKOV (10)
1
1.5
2
2.5
3
γ

FIG. 5

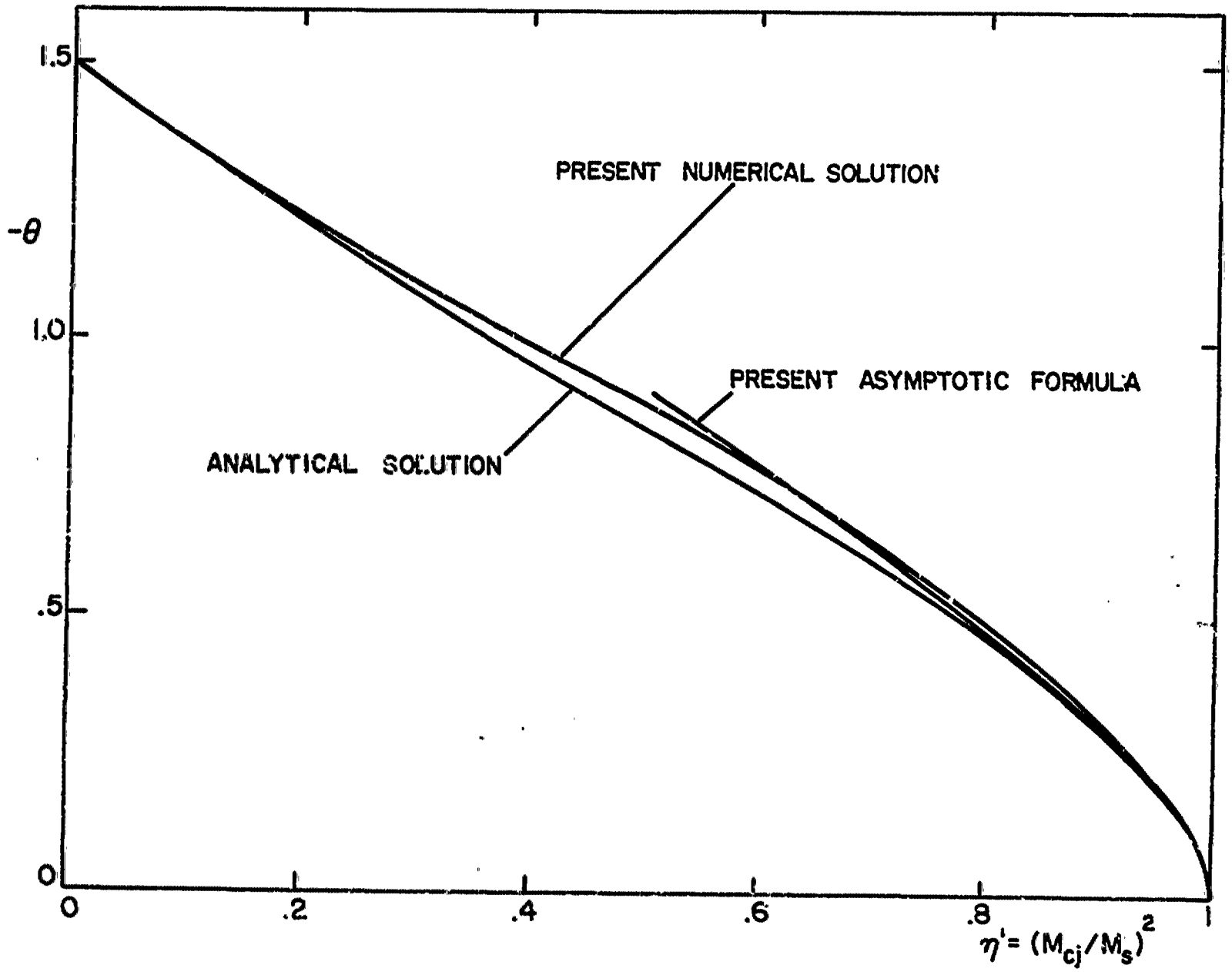
1.5
1.0
.5
0
$-\theta$
PRESENT NUMERICAL SOLUTION
PRESENT ASYMPTOTIC FORMULA
ANALYTICAL SOLUTION
0
.2
.4
.6
.8
1
$\eta' = (M_{cj}/M_s)^2$

FIG. 6

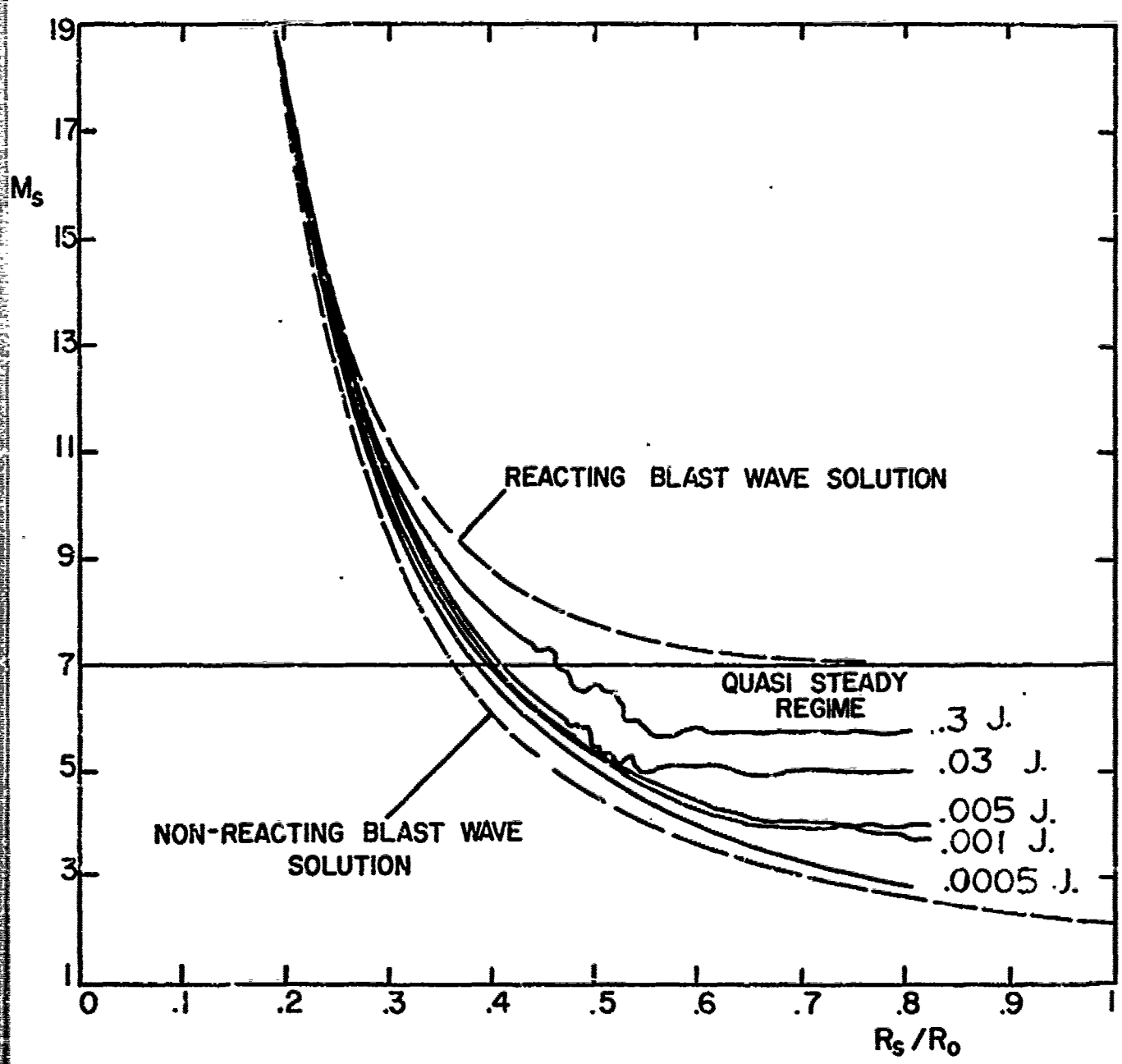
19
17
15
13
11
9
7
5
3
1
M_s
REACTING BLAST WAVE SOLUTION
QUASI STEADY REGIME
.3 J.
.03 J.
.005 J.
.001 J.
.0005 J.
NON-REACTING BLAST WAVE SOLUTION
0
.1
.2
.3
.4
.5
.6
.7
.8
.9
1
R_s/R_o

FIG. 7

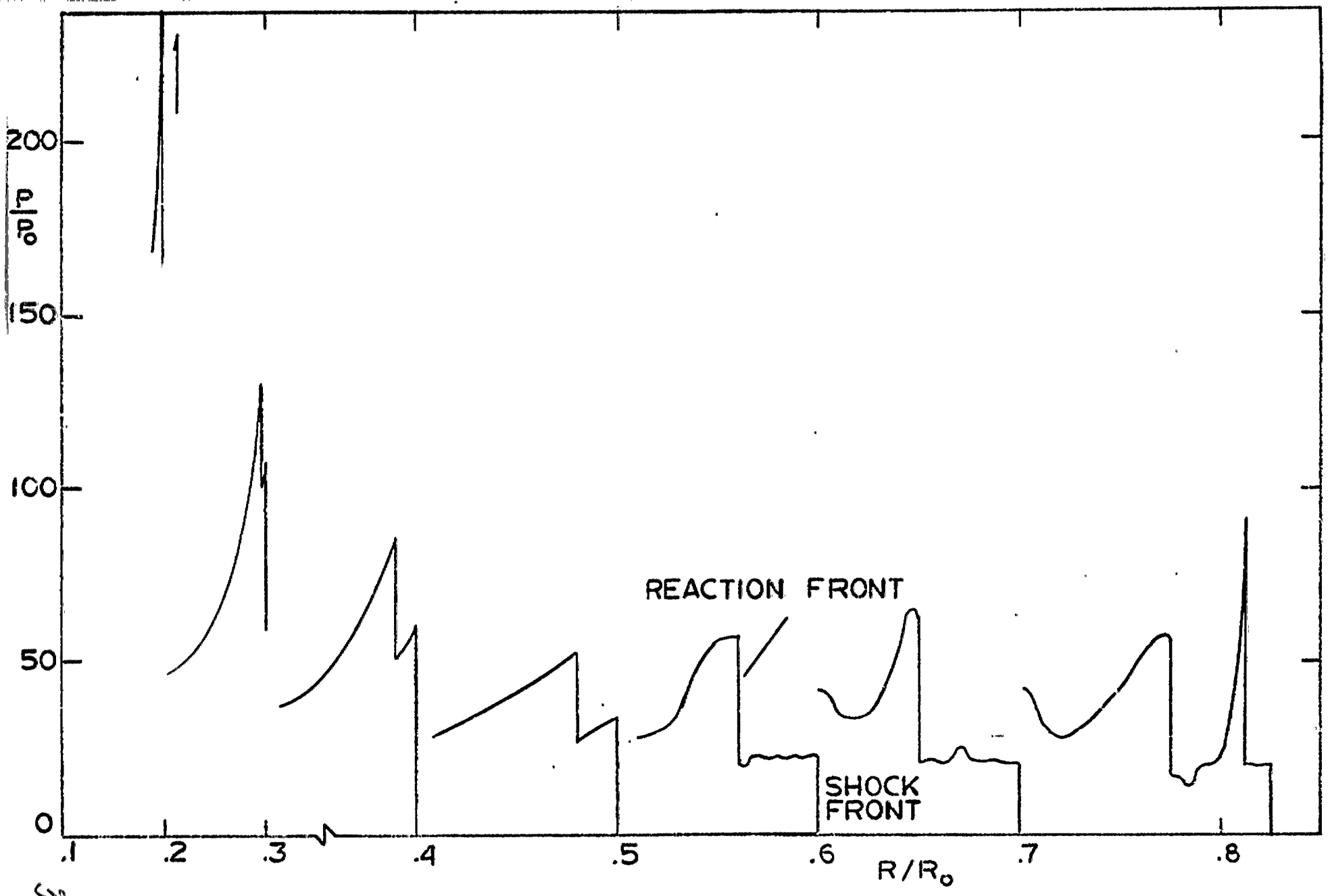
200
150
100
50
0
ρ/ρ_0
.1
.2
.3
.4
.5
.6
.7
.8
R/R_0
REACTION FRONT
SHOCK FRONT

FIG. 8

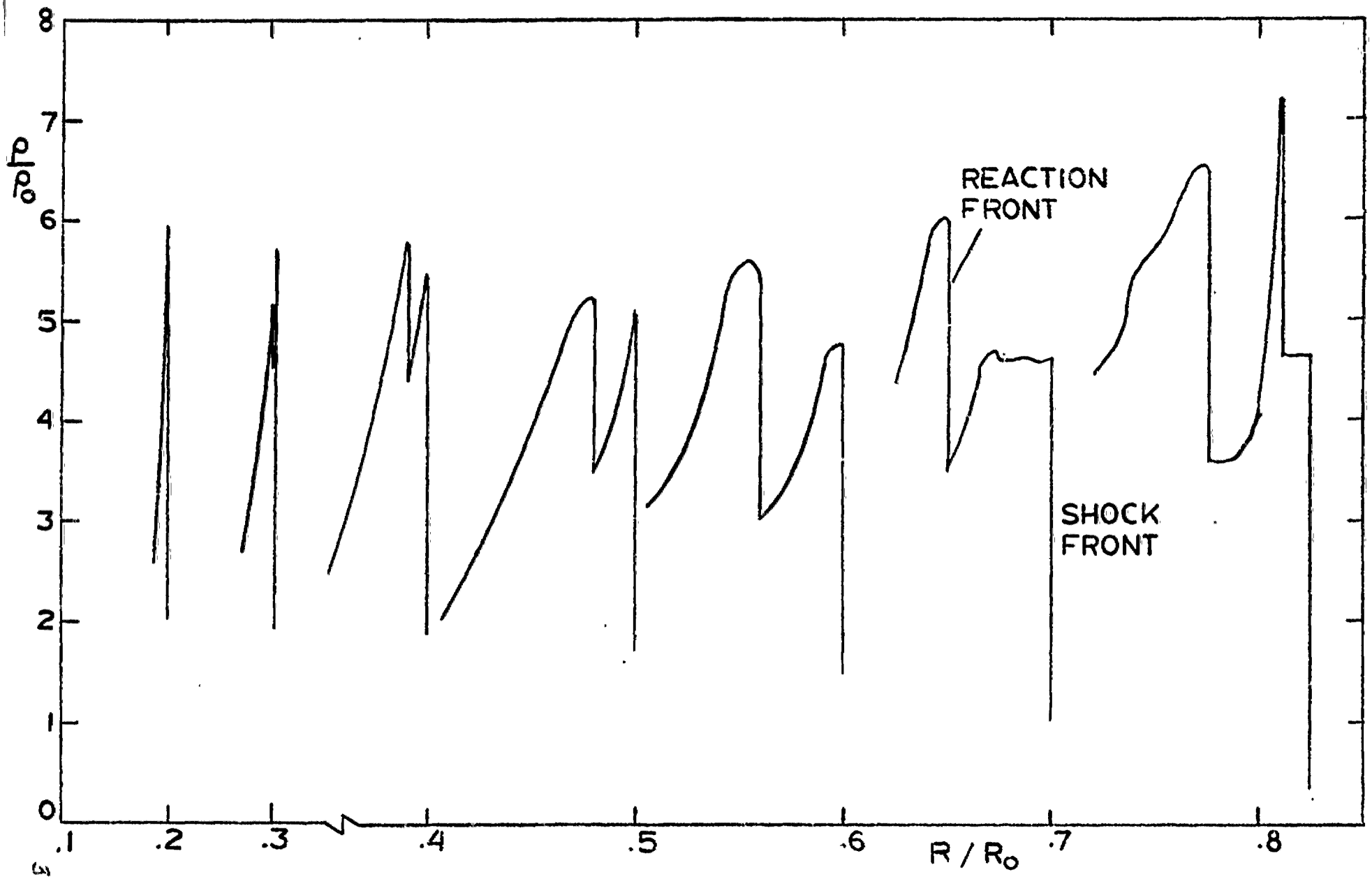
8
7
6
5
4
3
2
1
0
ρ/ρ_0
.1
.2
.3
.4
.5
.6
.7
.8
R/R_0
REACTION FRONT
SHOCK FRONT

FIG. 9

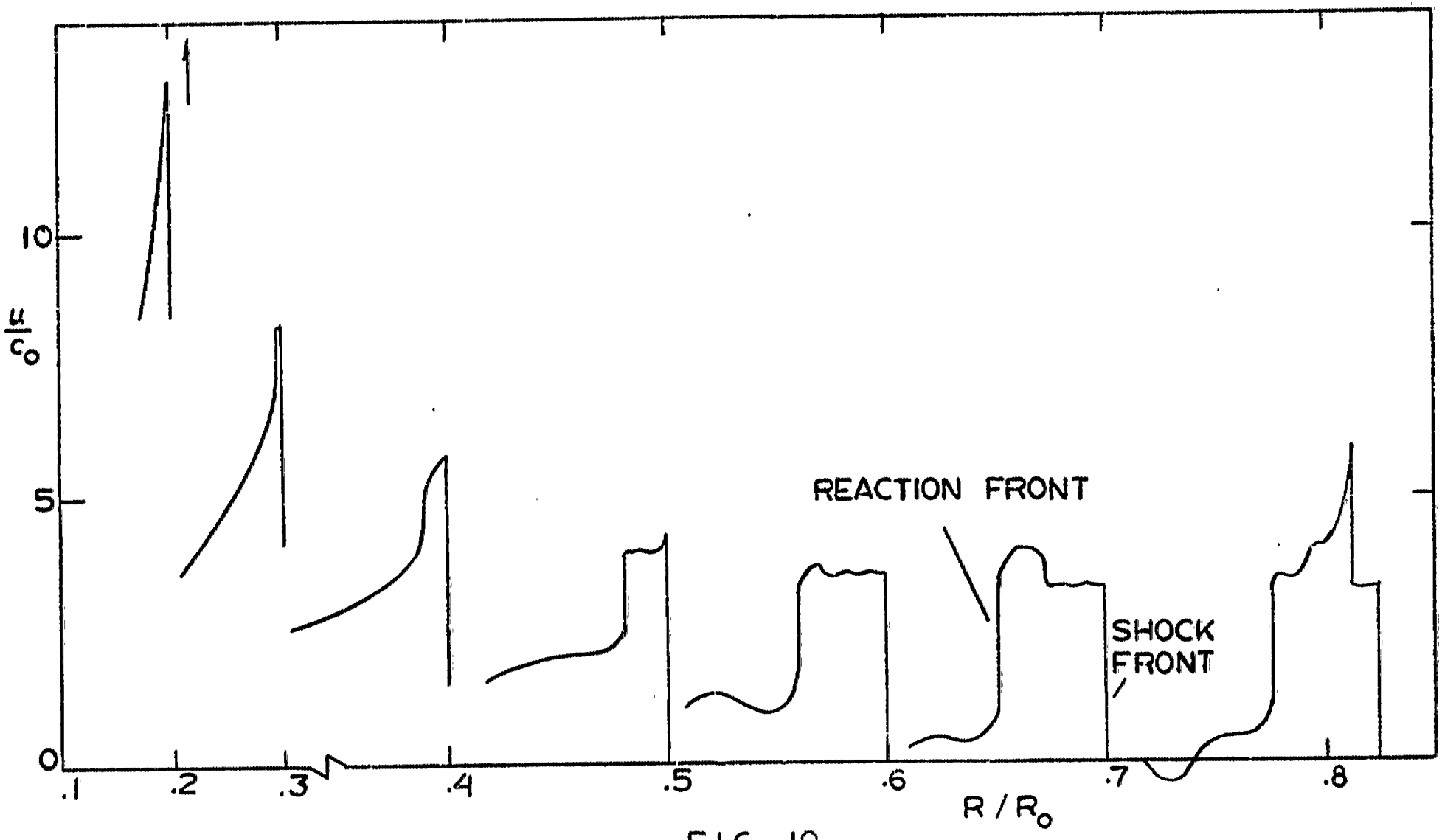

FIG. 10

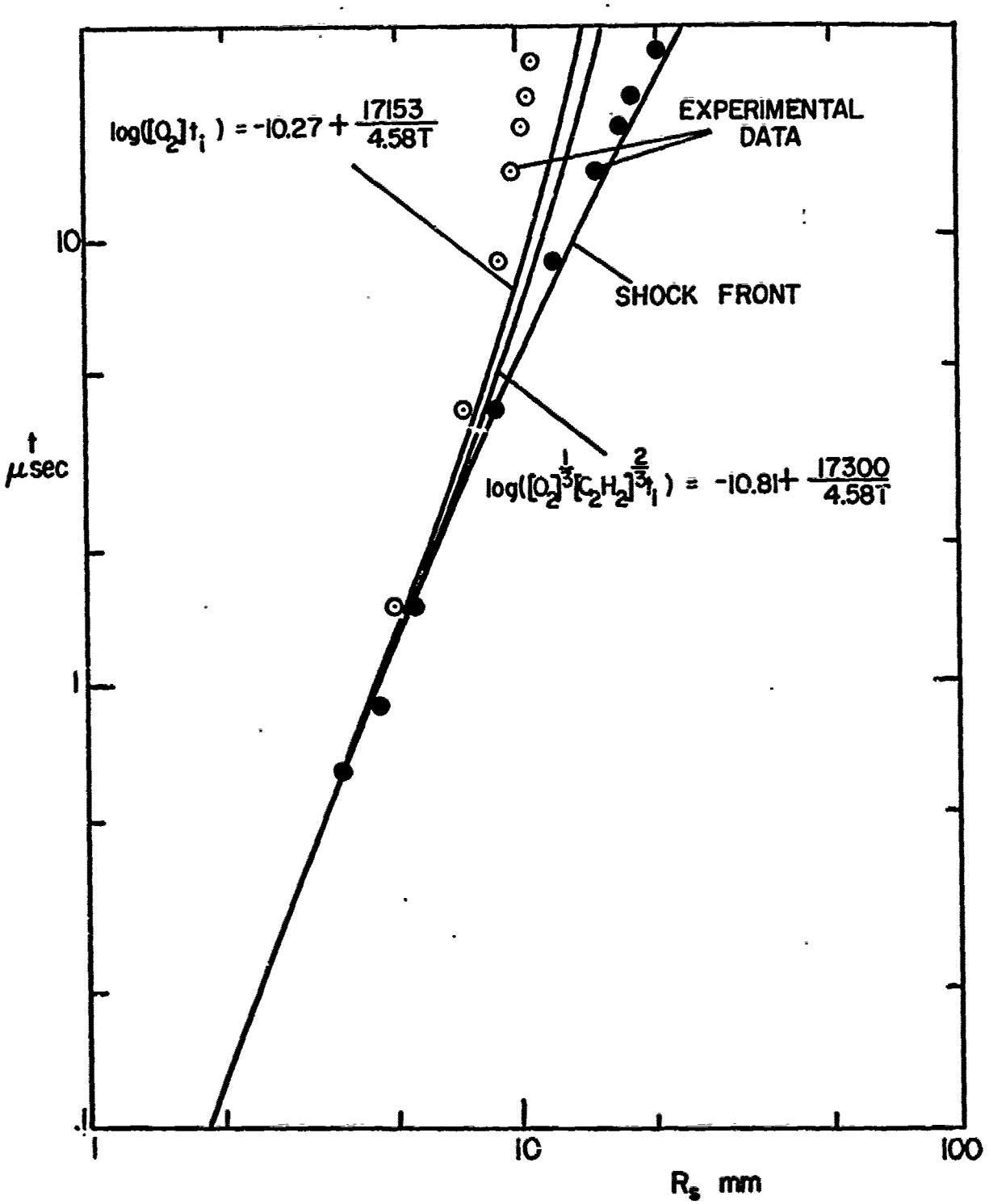
$\log([O_2]t_i) = -10.27 + \frac{17153}{4.58T}$
EXPERIMENTAL DATA
SHOCK FRONT
$\log([O_2]^{\frac{1}{3}}[C_2H_2]^{\frac{2}{3}}t_i) = -10.81 + \frac{17300}{4.58T}$
t
μsec
10
1
.1
1
10
100
R_s mm

FIG. 11

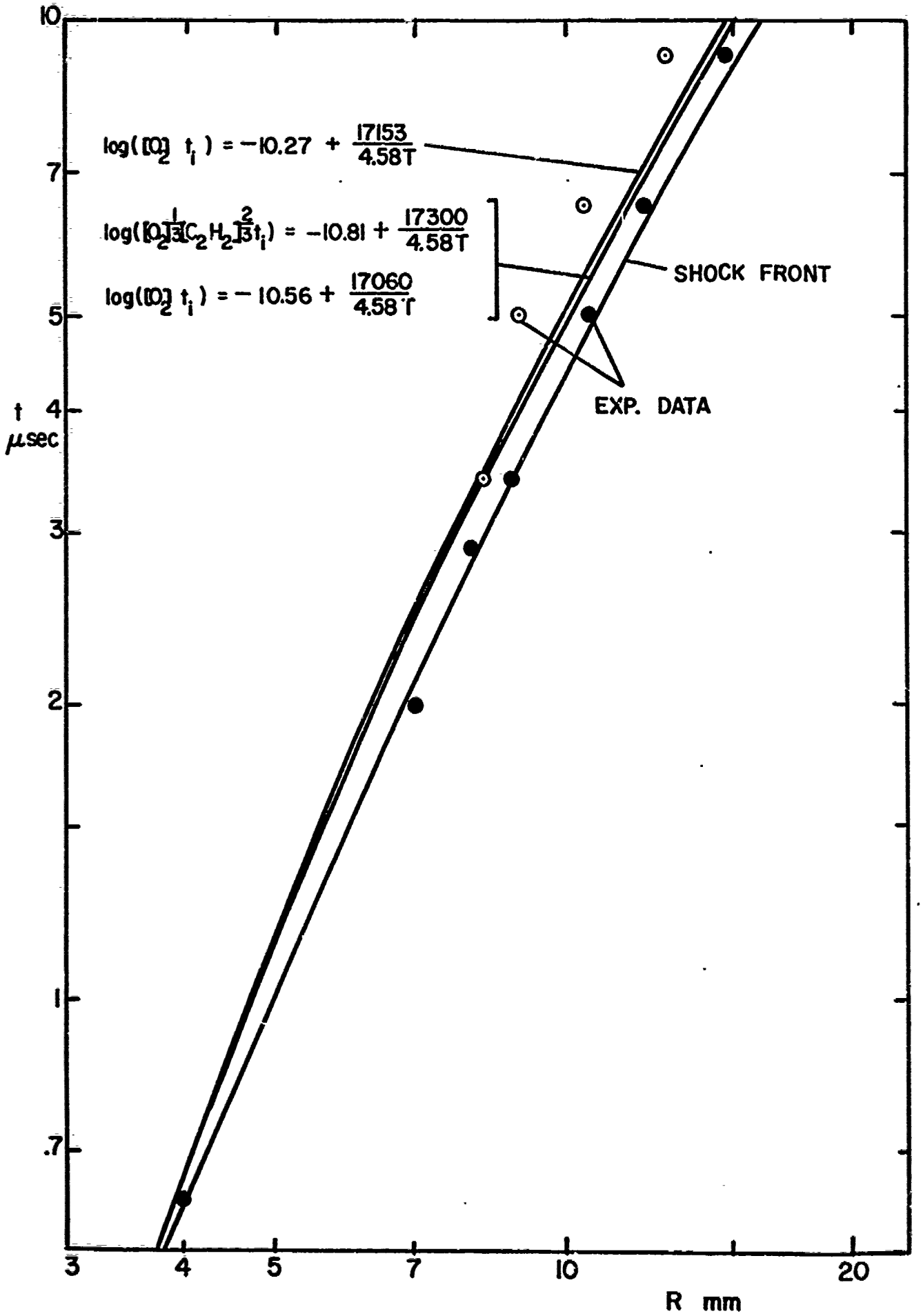
$\log([O_2]\, t_i) = -10.27 + \frac{17153}{4.58T}$
$\log([O_2]^{\frac{1}{3}}[C_2H_2]^{\frac{2}{3}} t_i) = -10.81 + \frac{17300}{4.58T}$
$\log([O_2]\, t_i) = -10.56 + \frac{17060}{4.58T}$
SHOCK FRONT
EXP. DATA
t μsec
R mm
10
7
5
4
3
2
1
.7
3
4
5
7
10
20

FIG. 12

42

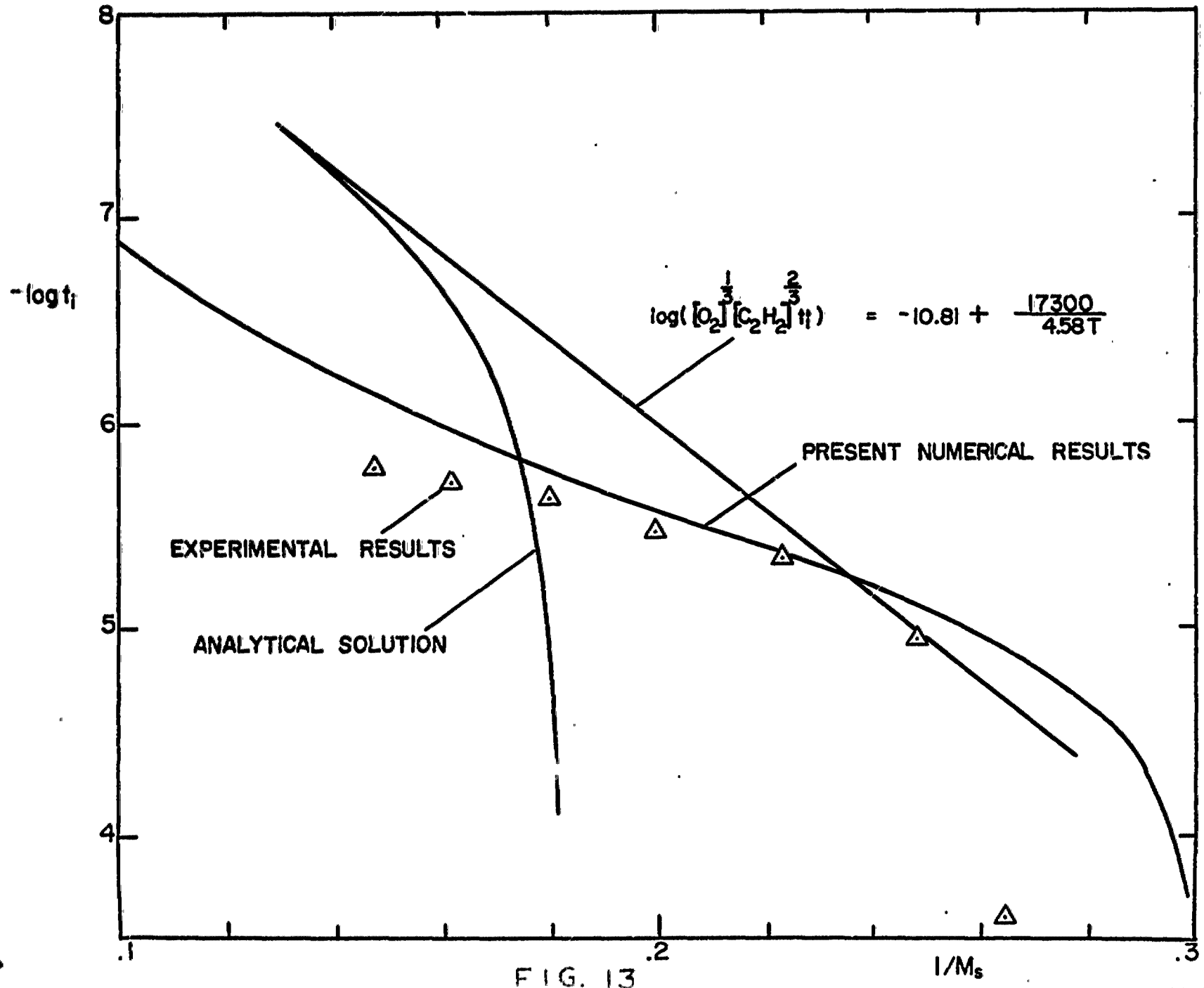
8
7
6
5
4
-log t_i
.1
.2
.3
$1/M_s$
$\log([O_2]^{\frac{1}{3}}[C_2H_2]^{\frac{2}{3}} t_i) = -10.81 + \frac{17300}{4.58T}$
PRESENT NUMERICAL RESULTS
EXPERIMENTAL RESULTS
ANALYTICAL SOLUTION

FIG. 13

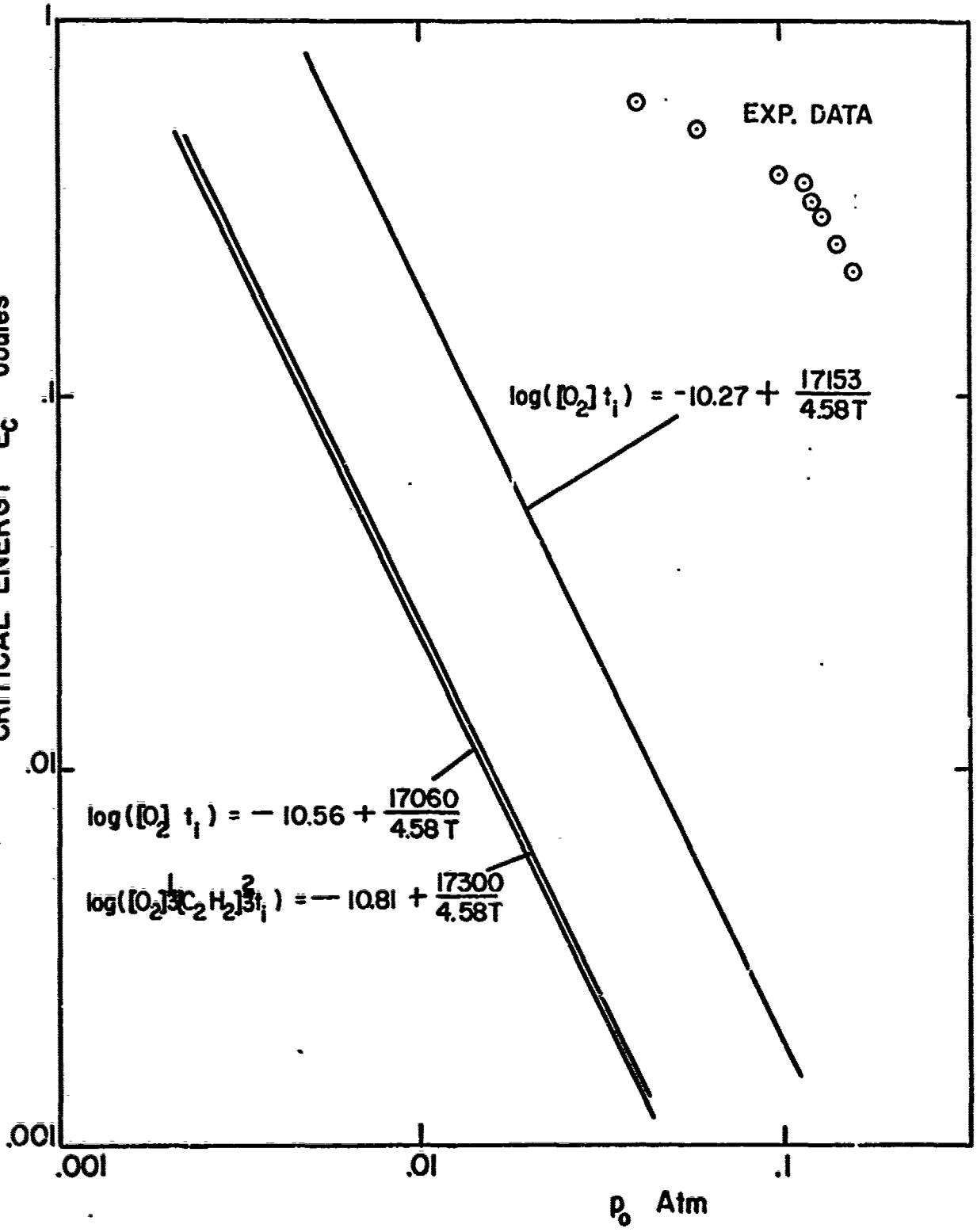
EXP. DATA
$\log([O_2]\,t_i) = -10.27 + \frac{17153}{4.58T}$
$\log([O_2]\,t_i) = -10.56 + \frac{17060}{4.58T}$
$\log([O_2]^{\frac{1}{3}}[C_2H_2]^{\frac{2}{3}}t_i) = -10.81 + \frac{17300}{4.58T}$
CRITICAL ENERGY E_c Joules
1
.1
.01
.001
.001
.01
.1
p_o Atm

FIG. 14

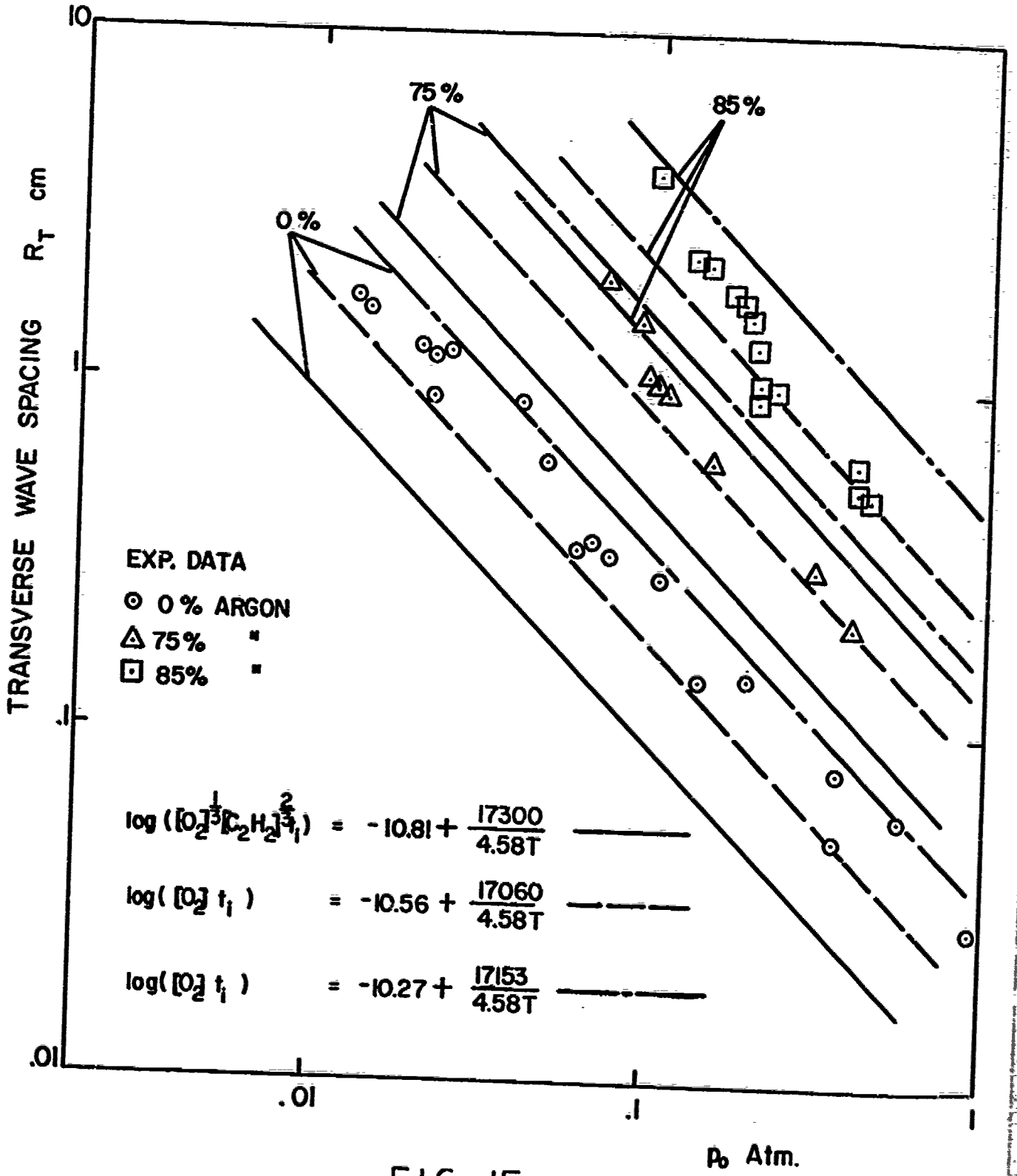
10
1
.1
.01
.01
.1
1
TRANSVERSE WAVE SPACING R_T cm
p_0 Atm.
0 %
75 %
85 %
EXP. DATA
⊙ 0 % ARGON
△ 75 % "
⊡ 85 % "
$\log([O_2]^{\frac{1}{3}}[C_2H_2]^{\frac{2}{3}}t_i) = -10.81 + \frac{17300}{4.58T}$
$\log([O_2]\,t_i) = -10.56 + \frac{17060}{4.58T}$
$\log([O_2]\,t_i) = -10.27 + \frac{17153}{4.58T}$

FIG. 15

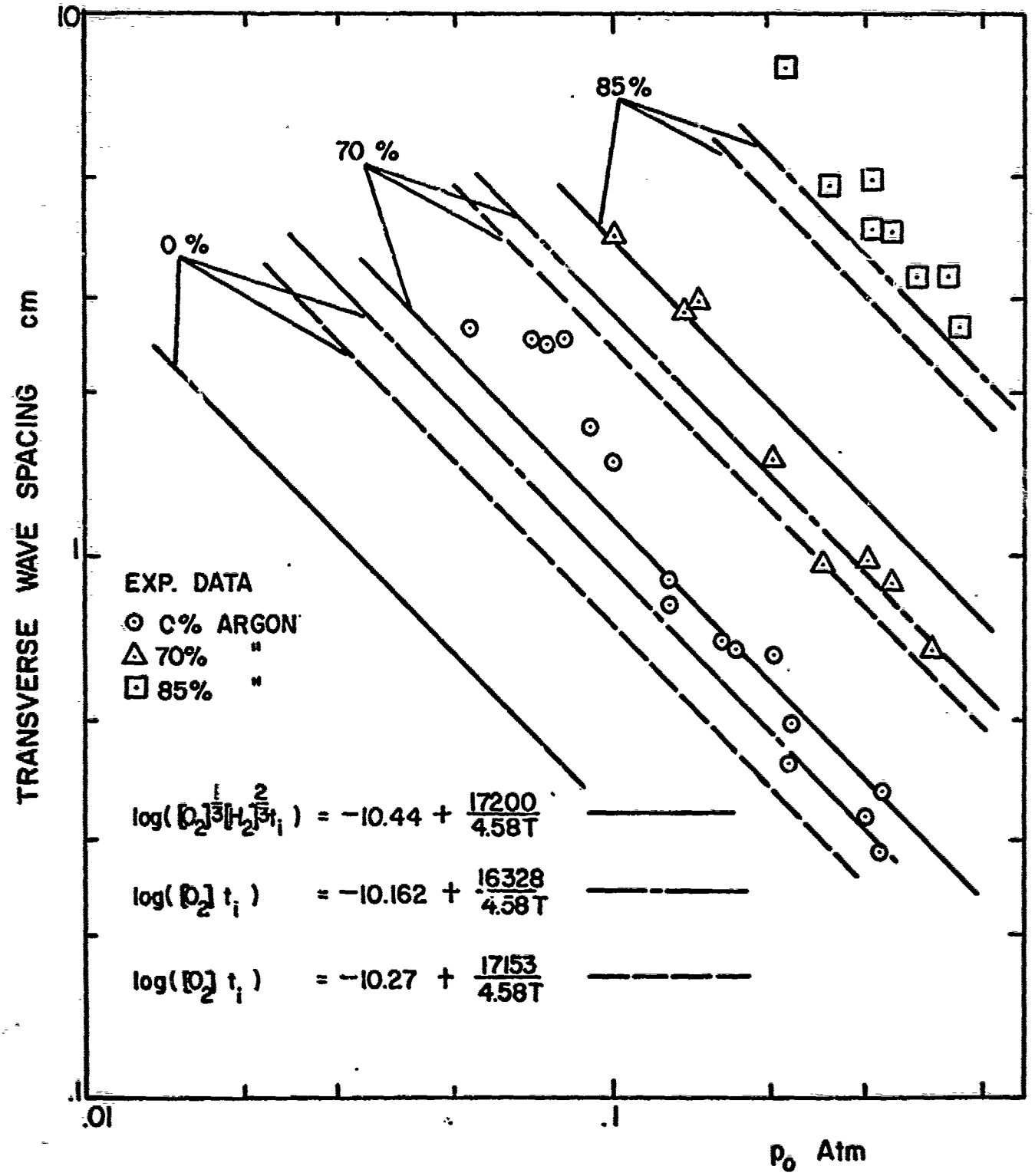
10
1
.1
.01
.1
TRANSVERSE WAVE SPACING cm
p_o Atm
0 %
70 %
85%
EXP. DATA
⊙ 0% ARGON
△ 70% "
⊡ 85% "
$\log([O_2]^{\frac{1}{3}}[H_2]^{\frac{2}{3}}t_i) = -10.44 + \frac{17200}{4.58T}$
$\log([O_2]\,t_i) = -10.162 + \frac{16328}{4.58T}$
$\log([O_2]\,t_i) = -10.27 + \frac{17153}{4.58T}$

FIG. 16

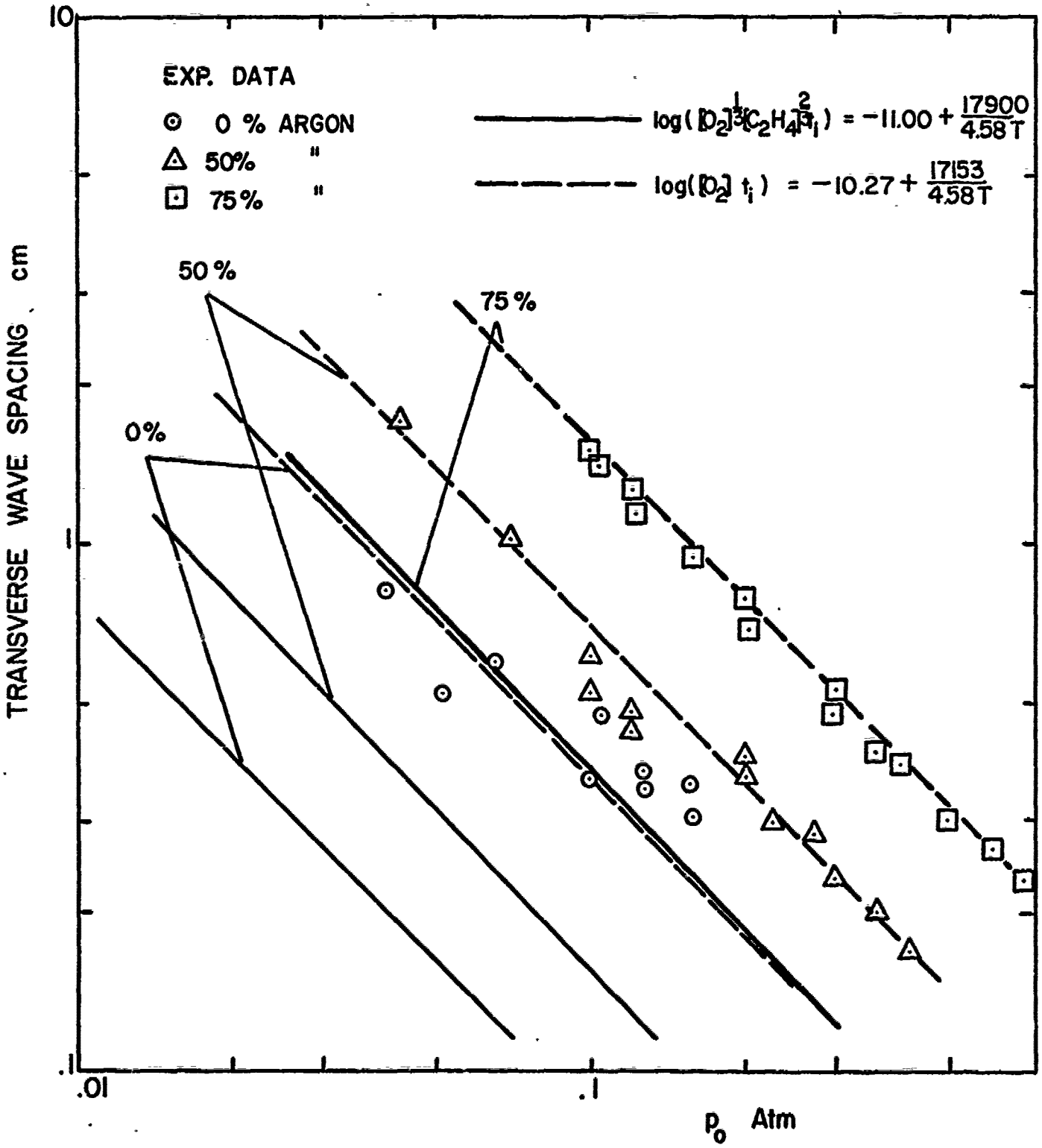
EXP. DATA
0 % ARGON
50% "
75% "
$\log([O_2]^{\frac{1}{3}}[C_2H_4]^{\frac{2}{3}}t_i) = -11.00 + \frac{17900}{4.58T}$
$\log([O_2]\,t_i) = -10.27 + \frac{17153}{4.58T}$
50 %
75 %
0%
TRANSVERSE WAVE SPACING cm
10
1
.1
.01
.1
p_0 Atm

FIG. 17